CHAPTER V

RESULTS AND DISSUSION

5.1 Matrix Characterization

5.1.1 Molecular weight characterization of base polymers

The molecular weight and the molecular weight distribution (PDI = Mw/Mn) of PC and ABS are important parameters in determining the mechanical, morphological, and rheological behaviors of PC/ABS blend and the pure polymers themselves. The Mw, Mn, and PDI of the each component in the blend are reported in Table 5.1.

GPC was also used to investigate potential degradation of PC by the metal salts which typically present in the ABS. They were known to degrade PC in the molten state during the melt blending in the extruder as reported by S. Balakrishnan and co workers. Figure 5.1 shows the GPC chromatograms of PC, ABS, and PC/ABS at weight ratio 40/60. Two peaks in the chromatogram were observed as clearly seen in this figure. The first peak, with a retention time of 20.6 min, was elucidated to be ABS whereas the second peak, with a retention time of 21.5 min, was found to be PC component in the blend. As the elution time of pure ABS and pure PC were 20.2 and 21.7 min respectively. From the figure, it can also be seen that the elution time of PC in PC/ABS blend do not change to the higher values. As a consequence, it can be infered that the molecular weights of PC in PC/ABS blend do not change to the lower value after blending. From these results, it can be concluded that the PC used in this system did not degrade after the blending process.

5.1.2 Mechanical properties measurement

Figure 5.2 shows the flexural modulus of PC/ABS as a function of PC content. The flexural modulus of the PC/ABS blends at various PC contents exhibited a positive deviation from the mixing rule. The highest modulus value of 2.66 GPa was observed in the blend system containing approximately 60 wt% of ABS and 40 wt% of PC. That value is higher than the flexural moduli of both the pure PC (2.4 GPa) and ABS (2.5 GPa). The positive-deviation phenomenon in the modulus of these alloys could also be seen in some previous works such as in the work of Lombardo et al. (1994) and Greco et al (1994). The existence of the inter-zones between the PC and ABS phases as discussed by Greco and coworkers was probably attributed to the very good adhesion at the interface between the two components. The authors hypothesized the invoked diffusion of low Mw species of SAN towards the PC domains resulting in certain compatibility between the SAN contained in the ABS and the PC itself. Figure 5.3 shows the flexural strength of the blend. The strengths of PC/ABS were found to increase with increasing PC in the blend from 72 MPa of pure ABS to 100 MPa of pure PC. In addition, the strength of PC/ABS blend exhibited negative deviation from the mixing rule up to about 60 wt% of PC and then turned to positive deviation from the rule for further addition of PC.

The tensile properties of PC/ABS blends are shown in Figures 5.4 and Figure 5.5. Figure 5.4 shows the variation of tensile modulus with PC content. From this graph, it can be seen that the tensile modulus also exhibited positive deviation and the highest modulus value of 2.06 GPa was observed in the blend system with approximately 40 wt% of PC, which is the same position with the flexural modulus. Whereas, the flexural moduli of pure ABS and pure PC were 1.92 and 1.86 GPa respectively. Figure 5.5 reveals the tensile strength of the blend. The strength increased with increasing PC in the blend from 46 MPa to 60 MPa of pure ABS and PC respectively. As seen in the figure, the increasing rate of tensile strength value was found to change at the composition between 40-60 wt% of PC in the blend. In addition, the strength quickly increased from 46 MPa of pure ABS to 54 MPa of the blend with 40 wt% of PC. For the further PC addition, the strength gradually increased to 60 MPa of pure PC. Moreover, elongation at break of the PC/ABS blends

shown in Figure 5.6 virtually unchanged up to 40 wt% PC. The breaking strains at these compositions were between 5-9 %. In the blends at the compositions with higher than 40 wt% of PC, the breaking strain rose sharply with the PC content and the maximum value of 55 % was found at the blend with 75 wt% of PC. After that, the breaking strain gradually decreased to 43% which is the value of pure PC. The variation of our breaking strain value corresponds with the result of B.S. Lombardo et al., 1994.

These remarkable behaviors of both flexural and tensile strengths of the blend involve with the phase transition. Normally, in the mixing of two immiscible polymers, two phase structure is usually formed. The component that occupy most volume of structure is called continuous phase and another phase is called dispersed phase. From Figure 5.3 flexural strength of the blend displayed negative deviation from the mixing rule up to about 60 wt% of PC. This region ABS was found to be a continuous phase because there is an ABS-rich phase and ABS also has lower viscosity than PC so ABS trends to be encapsulation species. For further addition of PC, the strength turned to be positive deviation from the rule of mixing, which this region PC performed as a continuous phase. The previous explanation can be clearly illustrated by Figures 5.7(a) to 5.7(f), which are morphologies observed on surfaces etched by a NaOH solution to remove the PC phase. We can see from this figure that up to 60 wt% of PC. The PC was observed as a dispersed phase in an ABS matrix, whereas at higher PC content, PC acted as a continuous phase dispersed by ABS domain.

As seen in Figures 5.2 and 5.4, both flexural and tensile modulus of the blend exhibited synergistic behavior. This behavior might be because of the low molecular weight fraction of ABS is able to dissolve in the PC domain resulting in certain compatibility between the SAN contained in the ABS and the PC itself and thus strengthening the ABS phase. This reason can be used to explain why the modulus of PC/ABS blends exhibited positive deviation from the rule of mixing.

5.1.3 Differential scanning calorimeter (DSC)

The previous explanation on the diffusion of low molecular weight species can be confirmed by interesting the glass transition temperature (T_g) of the blend. We have already known that the blends of miscible polymers usually exhibit only one T_g between those of the neat components. In the case of complete immiscibility, two T_g values can be detected which are the value of the two starting polymers. As a result of partial miscibility, the glass transition temperatures of the components will shift towards each other, which the magnitude of the shift depends on the reciprocal solubility of the phases in each other.

From Figure 5.8, we can see that all of our PC/ABS blend samples exhibited two T_g's of the PC-rich and ABS-rich phases. The T_g of PC was determined to be about 147°C whereas that of the ABS was 104°C. From the figure, T_g of the ABS-rich phase was found to shift to high value with an increasing amount of PC in the blends i.e. from 104°C of the ABS to 110°C in 75/25 mass ratio of PC/ABS blend or $\Delta T_g(ABS) = 6°C$. In the PC-rich phase, we observed a significant shift of its T_g value from 147°C of PC to 133°C in the blend containing 25/75 mass ratio of the PC/ABS or $\Delta T_g(PC) = 14°C$. The evidence of the shifts in T_g's of both phase thus confirmed partial miscibility of the two polymers. This phenomenon is attributed to the classical dilution effect due to the dissolution of the low Mw ABS species in the PC matrix and vice versa (Jiann-Shinc Wu et al., 1993). The difference in the T_g shifts when each phase are the dominant fraction is explained as due to more ABS dissolved in the PC-rich phase than did the PC dissolve in the ABS-rich phase causing the overall T_g shift i.e. the $\Delta T_g(ABS)$ to be less than $\Delta T_g(PC)$. The phenomenon was also observed by other workers (G. M. Hanafy et al., 2005; Jiann Shinc Wu et al., 1993)

The extent of miscibility/immiscibility of these PC/ABS blends was also assessed by using Fox Equation Eq. (5.1).

$$\frac{1}{T_g} = \frac{W_{ABS}}{T_{g\,ABS}} + \frac{1 - W_{ABS}}{T_{g\,PC}} \qquad (5.1)$$

The mass fraction of ABS in either the ABS or polycarbonate phase can be computed by this equation, which W_{ABS} is mass fraction of ABS in the blend. $T_{g\ ABS}$ and $T_{g\ PC}$ are the glass transition temperatures of pure ABS and PC respectively. Whereas T_g is the glass transition temperature observed for the phase of interest. The calculated values of the mass fraction of the PC in the ABS phase and those of the ABS in the PC phase were shown in Table 5.2. Based on the analysis using Fox relation, it confirmed our DSC experiments that polycarbonate is more soluble in the ABS than the ABS is in the polycarbonate. This behavior is also in good agreement with the analysis reported by Keitz et al. (1984).

5.1.4 Dynamic mechanical analysis (DMA)

Dynamic mechanical analysis (DMA) was utilized to characterize the neat polymers and all of the blends to get information about the miscibility and interaction between the blend components. Figure 5.9 illustrates the variation of dynamic storage modulus (E') of PC/ABS blends measured over the temperature range of 30 to 180 $^{\circ}$C. As the similar trend with flexural and tensile modulus observed in the previous experiments, the highest storage modulus of PC/ABS was also observed in the blend system containing 60 wt% of ABS and 40 wt% of PC with the value of 2.7 GPa. This value is higher than the storage modulus of both the pure PC (2.2 GPa) and ABS (2.4 GPa). The falling of storage modulus of PC/ABS blends in the DMA thermogram was observed to increase with increasing the amount of PC in the blend. In addition, the dynamic storage moduli of PC/ABS with PC content of 60 and 75 wt% were obviously seen to fall in two steps. The first step was between 110 and 120 $^{\circ}$C and the second was in the range between 130°C and 145°C. The falling of moduli corresponded with relaxation peaks of tan δ of the blends, which related with their glass transition temperature.

Glass transition temperatures of PC/ABS blends were also observed in the DMA thermogram based on the relaxation peaks of tan δ. Figure 5.10 shows tan δ of PC/ABS at various compositions. From the figure, we can see that all of our PC/ABS blend samples exhibited two relaxation peaks of tan δ which are the T_g's of the PC-rich and ABS-rich phases whereas the T_g, DMA of the pure PC was determined to be

about 150°C and that of the pure ABS was 110°C. This phenomenon can be attributed to the existence of two phases which are PC rich phase and the ABS rich phase as discussed previously. The relaxation at the upper temperature, which is the higher relaxation, results from the glass transition of PC rich phase, whereas, the lower relaxation likely results from the glass transition of ABS rich phase. Moreover, the transition temperature of each species in PC/ABS blend shifted toward each other, which is consistent with the DSC results. This result implies that low molecular weight fraction of ABS was migrated toward the PC-rich phase and vice versa. This is the reason why T_g of ABS is shifted to higher temperature. On the other hand, the T_g of the PC-rich phase is shifted to lower temperature from the pure PC and ABS. From the DSC and DMA results, we can conclude that these two components are partially miscible because the shift in their T_g's toward each other are observed.

5.1.5 High speed impact

The effect of PC content on high speed impact toughness of these PC/ABS blend systems was measured from the high speed puncher impact test. Figure 5.11 illustrates the relationship between the impact energy and the PC content in the matrix. Impact energy of PC/ABS blend exhibited percolation behavior which the energy rose immediately at a percolation threshold of 40 wt% of PC in the blend. The figure reveals that in an ABS continuous phase region and PC content up to 50 wt%, impact toughness slightly decreased with increasing the PC content in the blends. In this region, the lowest impact energy was found at 40 wt% of PC with the value of 2.5 J. After this region, the impact toughness of PC/ABS blends immediately increased when the PC mass fraction reaches to percolation threshold. The percolation threshold on high speed impact of our PC/ABS blend was found to be between 50-70 wt% of PC. After the percolation threshold of the blends, the high impact resistant region was observed with an impact energy range between 32-34.5 J. This region PC was observed as a continuous phase.

The impact result can be explained as the neat ABS normally has lower impact energy than the neat PC. Therefore, the PC/ABS blends with PC as a continuous phase show higher puncher impact energy than the blend having ABS as a continuous phase. In addition, in ABS continuous phase, dispersed PC might act as defects in the

bulk ABS and led to the decrease in the impact energy of the blend. From the puncher impact result, it is evidence that the blends reached the high impact toughness region when the PC acted as a continuous phase.

5.1.6 Thermal Stability Investigation of PC/ABS blend

The thermal degradation behavior of pure PC and ABS and PC/ABS blends at various compositions is presented in Figure 5.12. The degradation temperature at 5% weight loss is one parameter to determine thermal stability of polymers. From the figure, we can see that the degradation temperatures of pure PC and ABS at 5 % weight loss were 490 and 391°C, respectively and the degradation temperature of PC/ABS blends increased with increasing mass fraction of PC in the blend. This degradation behavior obeys the law of mixing. One benefit of blending PC into the ABS is thus to improve the thermal stability of the blend as a result of adding a high thermally stable specie into the blends. Moreover, the residual weight at 800°C of the PC/ABS blends was also found to increase with increasing PC mass fraction in the blend. The residual weights of pure PC and ABS were determined to be 20.8 and 0.15 respectively which are consistent with the values reported by Wen-Yen Chiang and Dao-Shinn Hwung (1987).

5.2 Determination of Processing Condition of PC/ABS-Kevlar Composites

5.2.1 Determination of processing temperature, time, and pressure

In this work, film stacking technique was used in PC/ABS composites fabrication. In this technique, temperature, pressure, and time of hot pressing used in a compression molder were the evaluated variables. The flexural strength and modulus values of the glass fiber-reinforced PC/ABS (60/40) as a function of temperature, pressure, and pressing time were examined for the optimal processing condition of the composites. Figure 5.13 shows the flexural modulus of the composites at various pressing temperatures under a constant pressing pressure and time, i.e. 15 MPa and 3 minutes. The result shows that the flexural modulus increases with the pressing

temperature. The maximum flexural modulus was obtained when the pressing temperature was higher than 260°C. The modulus values trend to be constant about 15 GPa when the processing temperature greater than 260°C. In addition, the flexural strength of the composites was found to increase with the pressing temperature up to about 150 MPa as shown in Figure 5.14. These behaviors suggested that the composite processed at higher temperature range used in this work will provide higher mechanical properties of the composites. The phenomenon is possibly due to the fact that the polymer matrix has the lowest viscosity above 260°C, which allows sufficient matrix wetting on the fiber. However, it is not recommended to use the processing temperature higher than the typical service temperature of Kevlar fiber, i.e. 230°C for long period of time and greater than 315°C for short period use [www. Aramid.com]. Consequently, the lower processing temperature of 200-220°C was chosen for the fabrication of these composites.

Since the properties of the composite in film stacking process can be affected by other processing parameters such as pressing time and pressing pressure, the ultimate mechanical properties can also be achieved by adjustment of these parameters. Figure 5.15 and 5.16 show the flexural modulus and strength of the composites processed at the temperature of 200 and 220°C at various times under a constant pressure of 15 MPa. The recommended processing temperature of PC, which requires the highest processing temperature in the blends, is between 190 and 230°C for thermoforming process and the like.(Richard C. Progelhof, 1993) From Figure 5.15, we can observe that the flexural modulus of both composites processed at 200 and 220°C gradually increase with the pressing time up to 30 minutes and reaches an optimal value of about 15 GPa after 30 minutes similar to that of specimen fabricated at high hot pressing temperature of 260°C for 3 min. Figure 5.16 illustrates the flexural strength of the composites as affected by the processing temperature and time. Initially, the strength of the composites linearly increases with the pressing time and also reaches to an optimal value using the pressing time greater than 30 minutes. The ultimate flexural strengths of the composite processed at 200 and 220°C were 100 MPa and 150 MPa respectively. This result suggests that the composite processed at 220°C can provide the maximum wetting of the matrix and gives the ultimate flexural strength similar to the value of the system processed at 260°C i.e. 150 MPa. These results imply that the required pressing time of at least 30 minutes at 220°C provides

maximum fiber wetting of the polymer melt and leads to the ultimate mechanical properties of the composite.

Another key parameter which might affect mechanical properties of the composite is the pressing pressure. Figure 5.17 and 5.18 show flexural modulus and strength of the composite processed at 220°C for 30 minutes using various pressing pressures. From the figures, modulus shows slightly increase and strength exhibits small decrease with the pressing pressure of 5-25 MPa. These results indicate that pressing pressure has only marginal effect on the flexural properties of the composites. However, to ensure that the composites achieve maximum wetting by the matrix when the Kevlar fabric is used, the hydraulic pressure of 2.5 kPa was selected as a processing condition used of our Kevlar-reinforced composites. As a consequence, it can be concluded that the optimal processing condition for the Kevlar-reinforced PC/ABS composites is 220°C for 30 minutes under pressure of 25 MPa.

5.2.2 Rheological behavior of PC/ABS blends as a polymer composite matrix

The melt viscosity at 260°C of PC/ABS blend as a function of PC content is shown in Figure 5.19. From the graph, we can see that PC/ABS blends at all compositions have lower viscosity than that of the neat ABS and PC. The neat PC and ABS have melt viscosity of 2,500 Pa.s and 1,900 Pa.s respectively. The lowest viscosity of the blends was found at 60 wt% level of the PC with the value of 1,000 Pa.s. The migration of the low molecular weight SAN specie into the PC phase and vice versa is hypothesized to lower the melt viscosity of the PC, the highest melt viscosity component in the blends. The migration has been reported to cause the viscosity of the blends to be lower than that predicted by the mixing rule (G. M. Hanafy et al., 2005; Keitz et al., 1984). In addition, the low molecular weight of the ABS migrating in to the PC molecular chains has been known to reduce the interaction between the PC molecules thus reducing the melt viscosity of the blends.

From the previous experiment, we already knew that the melt viscosity of the polymer matrix is one key parameter which affects the matrix wetting and the final

properties of the composite. In our composite fabrication, melt viscosity of each matrix had been fixed at the same value by varying the processing temperature of each matrix. Figure 5.20 shows the variation in viscosity of PC/ABS blends measured over the temperature range of 160 to 280°C. The figure reveals that the viscosity of the PC/ABS blends and also of the pure PC and ABS was found to sharply decrease in an exponential decay manner with an increase of the scanned temperature from 160°C to 280°C. At any temperature in the range of 160 to 220°C, the melt viscosity of the PC/ABS increased with the PC content. At the higher temperature, the melt viscosity of all blends approached the minimum values. From the result, we can see that in order to control melt viscosity of each matrix to be the same, the processing temperature of each system should be different from each other. In our composite processing, the melt viscosity of all matrices was controlled to be in the vicinity of 480 Pa.s which is the viscosity of the PC/ABS blends at weight ratio of 40/60 at 220°C. And the processing conditions of all matrices used are tabulated in Table 5.3.

5.2.3 Determination of optimum matrix content

Solvent extraction technique was used to determine the composition of constituents in the PC/ABS/Kevlar composites. Table 5.4 shows the measured density and the theoretical density of the composites with various matrix contents using PC/ABS blend at mass ratio of 60/40. The theoretical density of the composite predicted by the mixing rule increased with increasing the Kevlar fiber mass fraction due to the higher density of the fiber. However, in our composites, the high amount of the fiber in the composites led to the reduction of their measured bulk density. Figure 5.21 displays a comparison between the measured density and theoretical density of the composites at various fiber contents. From the graph, we can see that the measured density of the composite increased from 1.152 g/cm^3 to 1.192 g/cm^3 with increasing fiber content from 47.8 wt% to 73.1 wt%. This increase complies with the additivity rule. For higher fiber content, the measured density of the composite decreased with increasing fiber content due to not enough polymer to fully wet the fibers. This caused in void fraction in the composites and density of the composites thus decreased. Figure 5.22 depicts calculated void fraction of the composites at various matrix contents. It can be seen that the void fraction sharply decreased with

increasing matrix content up to 26.9 wt%. For further matrix addition, the void fraction in the composite slightly decreased and trended to be constant.

To determine the most optimal polymer matrix content in the composite, the various PC/ABS (60/40) films with varied thicknesses of 30, 40, 50, 100, 150, and 200 μm were used for film stacking processing in the composite fabrication. These obtained composite correspond to the PC/ABS matrix contents of 16.0, 19.2, 26.9, 33.4, 46.9, and 52.2 wt% respectively. Figure 5.23 reveals the flexural strength of Kevlar/PC/ABS composite as a function of the above matrix contents. As seen in the figure, the flexural strength sharply increases with the matrix content and then reaches the maximum value of 167 MPa at the matrix content of 33.5 wt%. After this content, the strength gradually decreases with increasing the matrix fraction. In addition, the flexural modulus of the composite as a function of matrix content also sharply increases with the matrix content and the highest modulus with the value of 15 GPa was acquired from the composite with the matrix content of 26.9 wt%. However, with increasing the matrix content beyond this ratio the modulus also decreases as shown in Figure 5.24. The sharp increase of the flexural strength and modulus is due to reduction of void content by increasing the quantity of polymer matrix to be able to penetrate into the Kevlar fabric as described in the previous experiment. This might lead to the enhancement of the interaction between the matrix and fiber. In the composite processing with the matrix content between 26.9-33.5 wt%, the polymer matrix was penetrated into the fabric ay the highest level and for a further increase in amount of the matrix, the mechanical properties decreased. The phenomenon is a good agreement with the mixing rule.

In order to obtain the optimum fiber content, both mechanical and ballistic properties of the composite were evaluated. As already described in the previous section, polymer matrix content in the range of 26-33 wt%, result in the highest degree penetration and wetting into the fiber and thus provided the maximum mechanical properties in the resulting composites. Dickson et al., 1998 and Park, 1996 suggested that for the best ballistic efficiency of polymer composite, the polymer matrix content is preferable to be in the range of 20-25 wt%. They also concluded that the composites with low matrix content have high penetration resistibility, whereas the high mechanical properties can be achieved at high polymer matrix content. To

balance between mechanical and ballistic properties of our Kevlar-reinforced PC/ABS composites in this study, the optimum fiber content selected to this study was approximately 70 wt% using 50 μm of PC/ABS film thickness.

5.3 Composite Characterizations

5.3.1 Mechanical properties measurement

The mechanical properties of fiber reinforced composite depend on several factors such as mechanical properties of the reinforced fiber and polymer matrix, the fiber volume fraction. One of the important factors is adhesion between the fiber and matrix. Figures 5.25 and 5.26 show flexural modulus and strength of Kevlar-reinforced PC/ABS composites as a function of PC content in the blend matrix i.e. at a fixed Kevlar content. It can be seen that the modulus of the composites was systematically increased from 7.6 GPa using pure ABS as a matrix to 13.8 GPa of the composite with pure PC as a matrix, as seen in Figure 5.25. From the prior experiment, PC/ABS blends exhibited synergistic behavior in flexural modulus so the blends moduli were higher than those of the neat PC and ABS. However, the synergism was not observed in the case of Kevlar-reinforced PC/ABS. This discrepancy might be due to the fact that for this Kevlar-reinforced PC/ABS system, the adhesion between the reinforcing fiber and the PC/ABS matrices could play a major in the composite flexural modulus. The flexural modulus curve in Figure 5.25 implies that the adhesion between the Kevlar and the PC/ABS matrices should increase with increasing PC content in the matrices. Figure 5.26 depicts flexural strength of the composites, which increased from 75 MPa using pure ABS as a matrix to 113 MPa of the composite with pure PC as a matrix. The increase of the flexural strength of the composites might be influenced by the interfacial strength between reinforced fiber and PC/ABS matrix and the flexural strength of the matrix itself.

5.3.2 Investigation of adhesion between Kevlar fiber and PC/ABS
matrices

In order to confirm the flexural results and to investigate the adhesion between the Kevlar fiber and PC/ABS matrices, peel strength of the composites had also been evaluated. Figure 5.27 illustrates the peel strength of the composites as a function of PC content in the matrix. As seen in the figure, the strength gradually increased from 3.9 N/cm of the composite using pure ABS as a matrix to 7.3 N/cm of the composite using pure PC as a matrix. This suggested that the interfacial adhesion between the Kevlar fiber and the polymer matrix could be improved by increasing the PC content in the matrix. The results also correspond with an increase of flexural modulus and strength with PC content as reported in the pervious experiment. The examination of the polarity of the PC/ABS matrices at varied composition of the blend was also performed for good understanding of their interaction with Kevlar. Figure 5.28 depicts variation in water contact angles of PC/ABS matrices at various compositions. In general, material with low water contact angle represents high polarity material and vice versa. From the figure, we observed a decrease of water contact angles of PC/ABS matrices from 104° of pure ABS to 88.4° of pure PC i.e. the polarity of the PC/ABS increases with increasing the PC content in the blend.

From the mechanical behaviors and the polarity of PC/ABS blend, it can be concluded that polarity of the Kevlar fiber (Solubility Parameter (δ) = 23) and the polycarbonate (Solubility Parameter (δ) = 21) trends to be closer to each other than that to of ABS (Mark, 1996). Therefore, the Kevlar-reinforced composite with greater PC content in the matrix exhibit higher compatibility between the fiber and the matrix. This is the reason why the peel strength and the flexural properties of the composite increased with increasing the PC content in the matrix.

5.3.3 Thermal stability investigation of Kevlar-reinforced PC/ABS

The thermal degradation of Kevlar-reinforced PC/ABS composite is presented in Figure 5.29. The TGA thermograms of all composites were found to decrease in two steps. The first step was between 390 and 490°C and the second step was

approximately 560°C. The decreasing of TGA thermogram corresponds with the decomposition of polymer matrix and Kevlar reinforced fiber. The weight reduction at the lower temperature range results from degradation of polymer matrix. From the figure, it can be seen that the degradation temperature at 5% weight loss increased with increasing PC content in the matrix as seen in the degradation temperature of PC/ABS blends. In addition, the degradation temperature of the polymer matrix of the composites was close to the value of pure polymer and ABS blends measured from the previous section. The weight reduction at the higher temperature range results from degradation of Kevlar reinforced fiber which all composites exhibited nearly the same value of 560°C. Moreover, the char yields of all composites were found to be about 40 wt%. This value consisted of residue from the polymer matrix and the Kevlar fiber. The TGA thermogram of the composites could also be used to determine the fiber and matrix content. From the TGA calculation, the matrix contents of all composites were about 20-23 %wt. These value were close to the values calculated from the solvent extraction test listed in Table 5.4.

5.4 Ballistic Impact Test of the Kevlar-reinforced PC/ABS Composite Armors

5.4.1 Low level ballistic impact test

Twenty piles of Kevlar composites at various PC/ABS compositions (i.e. 10/10 panel arrangement) were used for the ballistic impact test using 9 mm hand gun with a standard gain of a round lead projectile having lead outer coating to evaluate the most effective composition of the matrix for ballistic protection. Interestingly, the projectile could be stopped in all of the composite targets. Those ballistic impact test results are shown in Table 5.5a and 5.5b. However, at close evaluation, the firing results indicated that the composite using the pure PC and 25/75 mass ratio of PC/ABS matrices had lower penetration resistance since their front plates were penetrated by the projectile. Figure 5.30 shows diameter of delaminated area of the composites after ballistic impact at various matrix compositions. Additionally, from the study of Naik et al. in 2005, they found that the projectile kinetic energy absorbed by matrix delamination is important next to the reinforced fiber failure mechanism.

The quantity of the matrix delamination of our fired composite was evaluated by measuring a diameter of the delaminated area. The results revealed that the composites with less than 25 wt% of PC in the matrices gave a relatively large delamination area which increased with the PC content in the matrix and reached to the maximum value (63.3mm) at 25 wt% PC. With increasing the PC content, the delamination area was found to be decreased. The interfacial strength between the matrix and the fiber and the capability to spread out impact energy of the composite are important factors affecting the delamination area of the composite. The interfacial adhesion between the Kevlar fiber and the polymer matrix was proved to increase with the PC content in the matrix as determined from the contact angle results. The higher adhesion between the fiber and matrix at an increased PC content in the matrix will restrict the delamination of matrix and fiber. This is the reason why the delamination area of the after fired composites decreased with increasing PC content in the matrix when the composite with higher than 25wt% of PC in the matrix was used. As described in Chapter 2, the higher the wave velocity, the greater the volume of material can interact with the projectile. The value can be used to further clarify the impact failure of the samples. In theory, the velocity of wave propagation increases with the square root of material's modulus and decreases with the square root of material's density as shown in the Equation 5.1.

$$V_S = \sqrt{E/\rho} \qquad (5.1)$$

when $\qquad E \qquad$ = modulus

$\qquad\qquad V_S \qquad$ = wave velocity

$\qquad\qquad \rho \qquad$ = density

The wave velocities of the composites at various matrix compositions were calculated and shown in Table 5.6. From the table, it can be seen that the wave velocity of the composite using ABS as a matrix exhibited the lowest wave velocity value which indicated that the composite has low capability to spread out the ballistic energy. The lack of this capability of the composite led to the lower the volume of the material to interact with the projectile (Kroschwitz, 1991). This characteristic

explained the low delamination area of the composite with less than 25 wt% of PC in the matrix.

In the final stage of this low level ballistic impact test, the residual kinetic energy of the projectile absorbed by the clay witness was evaluated by measuring damage volume of the clay as shown in Table 5.7. From the table, we can see that the lowest damage volume of the clay was observed in the composite with 40 wt% of PC in the matrix. The lowest damage volume of the clay was 31.5 cm^3 whereas the damage volume of the clay of the composite with pure PC and ABS were 41 cm^3 and 42.5 cm^3 respectively. As explained in chapter 2, the delamination between the reinforced fiber and polymer matrix has been known to be one of the most important energy absorption mechanisms in ballistic impact. In the case of composite with 40/60 PC/ABS matrix, the highest energy absorption might be because of the optimal adhesion between the Kevlar fiber and the PC/ABS matrix. High adhesion between reinforced fiber and polymer matrix provides composites armor to give high modulus and also high wave velocity. These lead to high capability to spread out impact energy and high volume of composite interacting with the projectile. However, too strong adhesion between the fiber and the matrix, the longitudinal wave velocity in the Kevlar fiber can be reflected at the rigid adhesion point (Kroschwitz, 1991), which results in high strain gradient and low energy transferring along the fiber. As a consequence, too strong adhesion or too high PC content in the matrix results in lower energy absorption of the composites. In the other hand, with too weak adhesion between the Kevlar fiber and the PC/ABS matrix, the composite will exhibit rather low modulus and also low wave velocity. In this case, the composite will have low capability to spread out ballistic energy and the delamination area also decreases. These behaviors cause the result in low energy absorption of composite due to low adhesion between fiber and composite.

To confirm the results of low level ballistic impact test, peeled surface morphologies of the composites were examined using SEM. Figures 5.31a and 5.31b depict surface morphology of the composite with the ABS as a matrix. The composite exhibited high degree of interfacial failure implying that the fibers were easily stripped from the matrix material. It means that the adhesion between the Kevlar fibers and the ABS matrix is very poor. In Figure 5.31e and 5.31f, the composite with

the pure PC as a matrix showed good adhesion between the Kevlar fiber and the matrix. This composite exhibited low interfacial or adhesive failure but rather high matrix failure i.e. cohesive failure. However, the composite with 40 wt% PC in the matrix displayed substantial degree of both matrix failure and interfacial failure. Moderate amount of stripped fibers was observed in this composite as illustrated in Figure 5.31c and 5.31d. Because of suitable adhesion between the fiber and matrix, the composite with 40 wt% of PC in the matrix should provide optimal wave velocity to spread out ballistic energy whereas the composite adhesion point was not too strong to reflect the wave velocity, hence, its impact energy can be effectively transferred along the fiber. These results explained why the composite with 40 wt% PC matrix exhibited the highest ballistic efficiency. From the above results, we can conclude that the Kevlar-reinforced 40/60 PC/ABS exhibited optimal level of interfacial interaction between the Kevlar fiber and the PC/ABS matrix for ballistic resistance.

5.4.2 Ballistic impact test of NIJ level III-A

In this investigation, the Kevlar-reinforced 40/60 PC/ABS composite samples with the combined thickness of 40 piles, 50 piles, and 60 piles were subjected to a ballistic impact evaluation at a projectile velocity required by NIJ standard for Level III-A. From the previous research, we have already known that specimen's thickness and arrangement of the composite panel are important factors for the ballistic performance of ballistic composite (S. pathomsap, 2005). The composite having at least 50 piles of the Kevlar cloth with areal density 0.24 g/cm^2 in 10 piles/panel can protect the ballistic impact at level III-A. They also found that the 30-ply panel of the composite should be placed in the front face of the composite panel assembly to yield the best ballistic resistance. In addition, the ballistic energy will be dissipated via the inertial effect when the projectile passes through the gap between two plates of the composite (S. pathomsap, 2005).

Our composite samples were approximately 2 mm in thickness having 10 piles/panel, 4 mm, 6 mm and 8 mm in thickness in 20 piles/panel, 30 piles/panel and 40 piles/panel composites respectively. The areal density of the composite was determined to be 0.23 g/cm^2 in 10 piles/panel composite. In order to obtain the most

appropriate number of piles of the composite to protect ballistic impact at level III-A, the samples with combined thickness of 40, 50 and 60 piles were prepared. The composites with combined thickness of 50 and 60 piles had one type of arrangement, i.e. 30/10/10 and 30/10/10/10 configurations respectively, whereas the sample with combined thickness of 40 piles had two types of arrangement i.e. 30/10 and 40/0 configurations.

The results obtained from NIJ level III-A ballistic impact test are shown in Table 5.8. All samples were fired with .44 Magnum 240 grains with impact velocity about 426 m/s. The deformation depth and diameter of the clay witness were measured. As shown in the table, both composites with the combined thickness of 40 piles cannot pass this level of NIJ standard for ballistic protection. It indicates that the composites with combined thickness of 40 piles possessed insufficient energy absorption for stopping the level IIIA projectile. As seen in the table, the deformation depths and diameters of the clay witness of the composites with the combined thickness of 50 piles, and 60 piles were measured. The results revealed that the deformation diameters of the clay expectedly decreased with increasing the number of piles of the composites and the deformation depth also exhibited the similar trend. This is an because the composite with the greater number of piles will have higher impact energy absorption capability. The high impact energy absorption of the composite led to low residual impact energy of the projectile transferred to the clay witness. Consequently, the diameter and depth of the clay were found to decrease with increasing the number of piles of the composite. Form this ballistic result, it can conclude that the suitable number of piles of the composite to protect ballistic impact at level III-A is 50 piles.

In order to observe the effect of arrangement of the composite panel to the ballistic resistant efficiency, the samples with combined thickness of 50 piles were prepared with varied type of arrangement, i.e. 20/10/10/10, 30/10/10, 40/10, and 50/0 configurations. These samples were also fired with .44 Magnum at the same grain and velocity (NIJ level IIIA). The deformation depth and diameter of the clay witness of the composite were shown in Table 5.9. From the table, it revealed that the damage areas of the samples with an arrangement of 30/10/10, 40/10, and 50/0 were not significant to each other but they exhibited much better ballistic performance than that

of 20/10/10/10. It was clearly demonstrated by the lower diameter and depth of the clay witness of the composite with 30/10/10, 40/10, and 50/0 arrangement than that of 20/10/10/10. This result is consistent with the study of S. Pathomsap (2005), which can be explained that the composite with 20/10/10/10 arrangement has insufficient mechanical integrity to destroy the projectile, which leads to higher impact energy can still transfer to the adjacent plate and cases the higher diameter and depth of the clay witness of this composite compared with that of the other composite. From all above results can be concluded that at least 30 piles of the composite should be placed on the front face to deform the bullet and yield the best ballistic efficiency. Moreover, for the composites with sufficient mechanical integrity of their front faces, the arrangement of the composite panel does not effect to their ballistic resistant efficiency.

Table 5.1: Mw, Mn, and PDI of PC and ABS used in this research

Component	Mw	Mn	PDI
PC2800	50482	27571	1.83
ABS	105251	51052	2.06
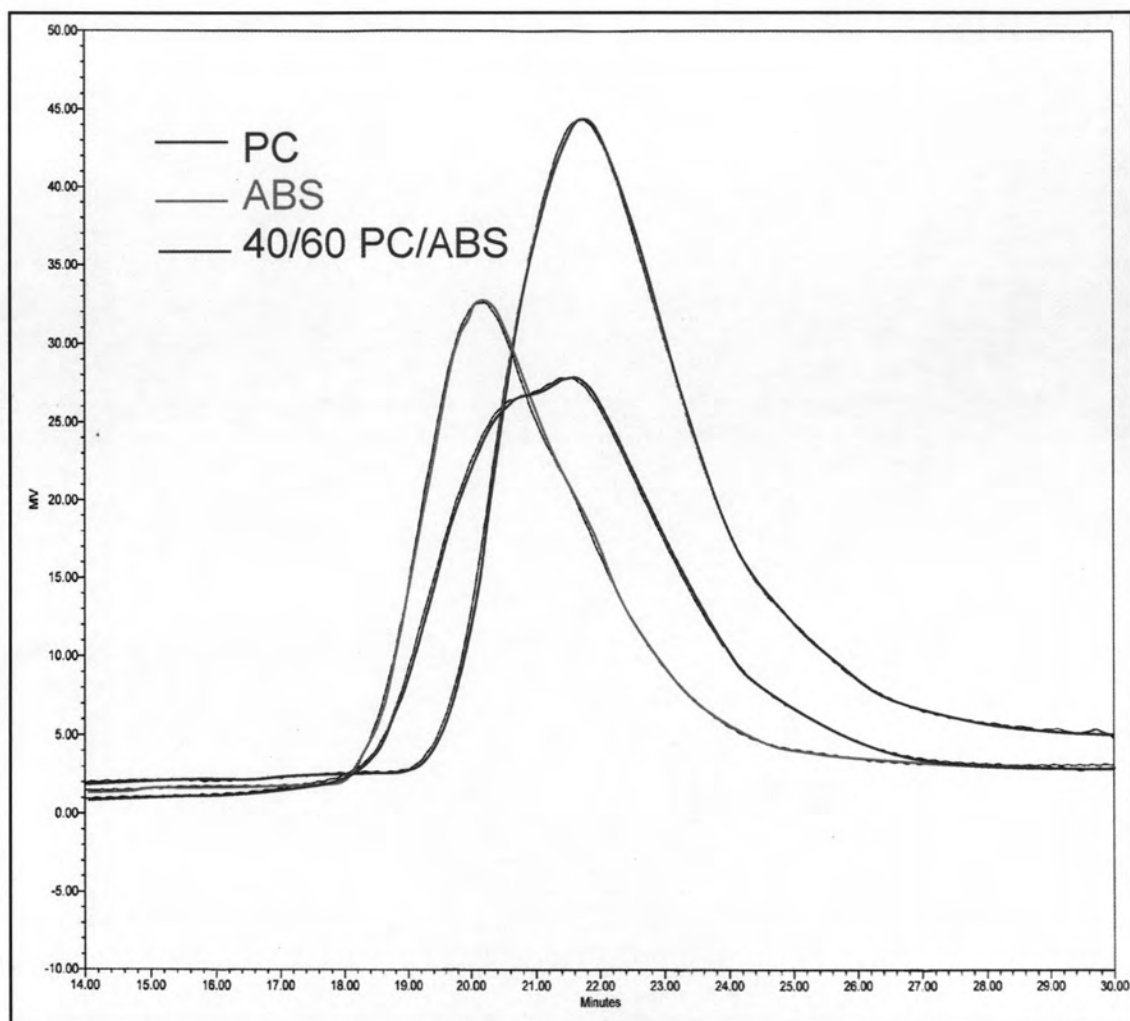
Figure 5.1: GPC chromatograms of PC, ABS, and PC/ABS at weight ratio 40/60.
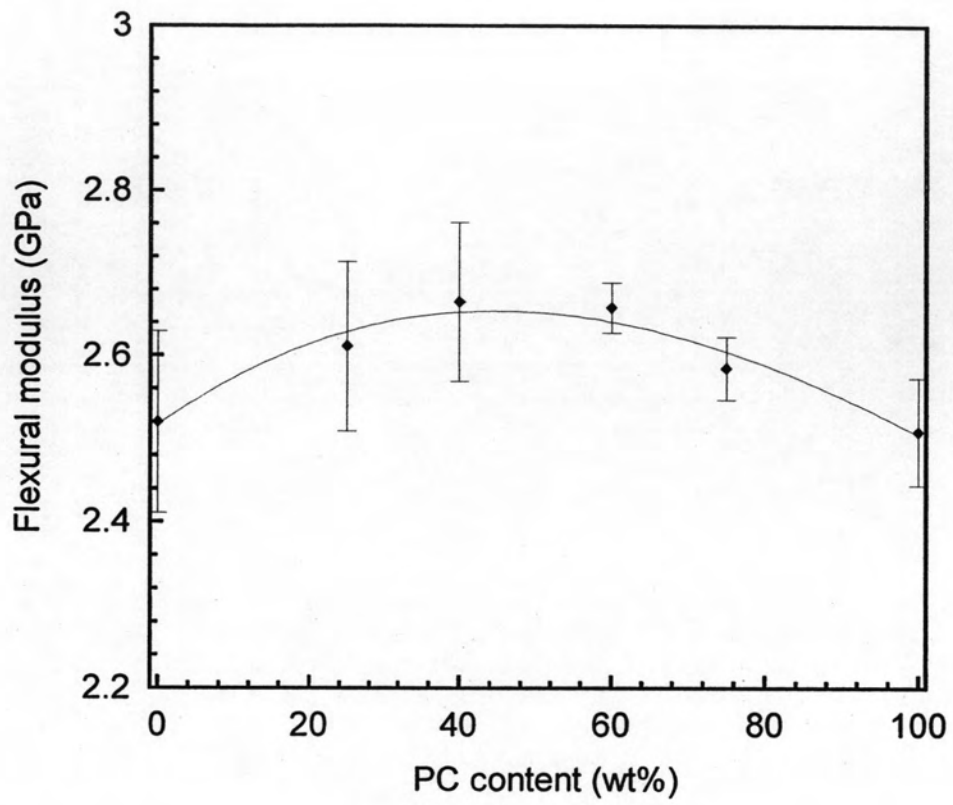
Figure 5.2: Flexural modulus of PC/ABS blends as a function of PC content
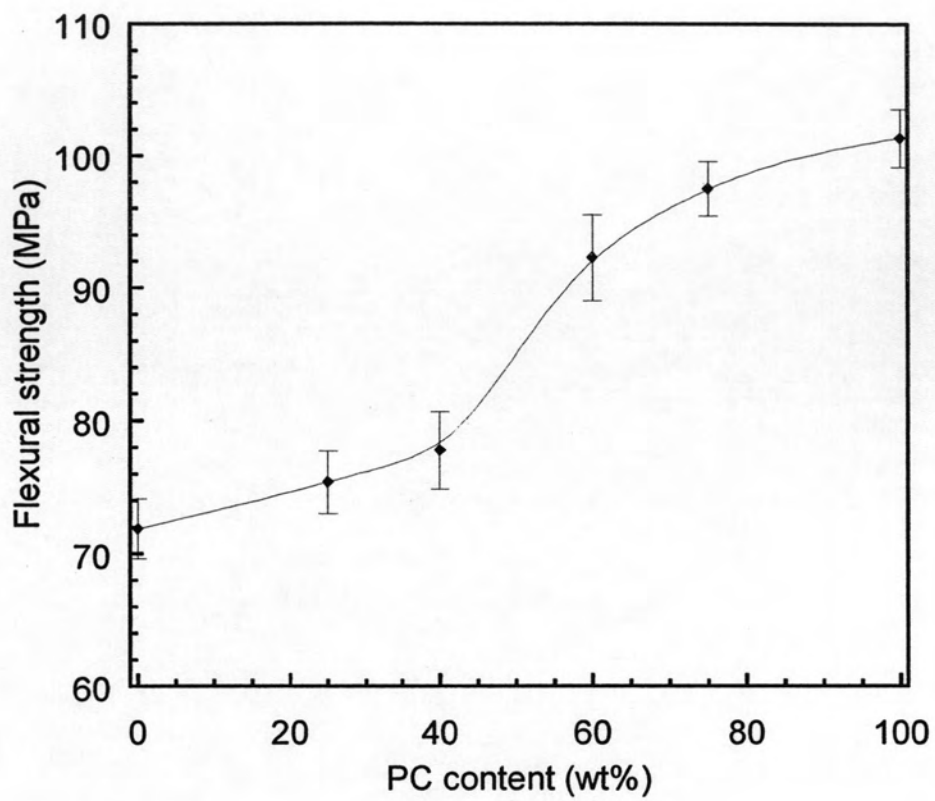
Figure 5.3: Flexural strength of PC/ABS blends as a function of PC content
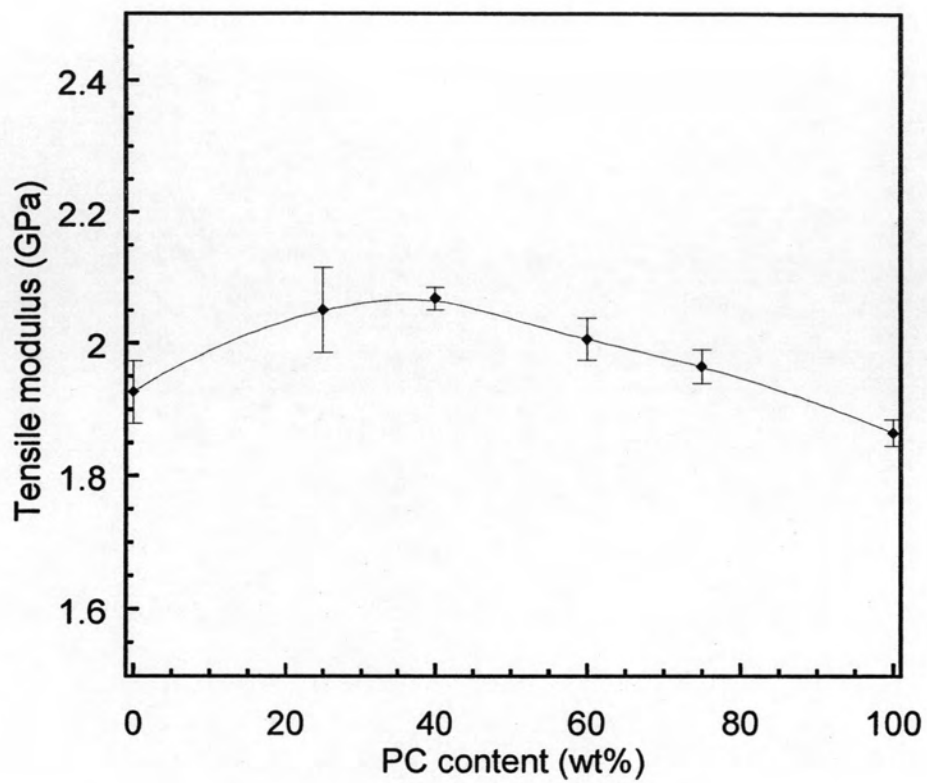
Figure 5.4: Tensile modulus of PC/ABS blends as a function of PC
content
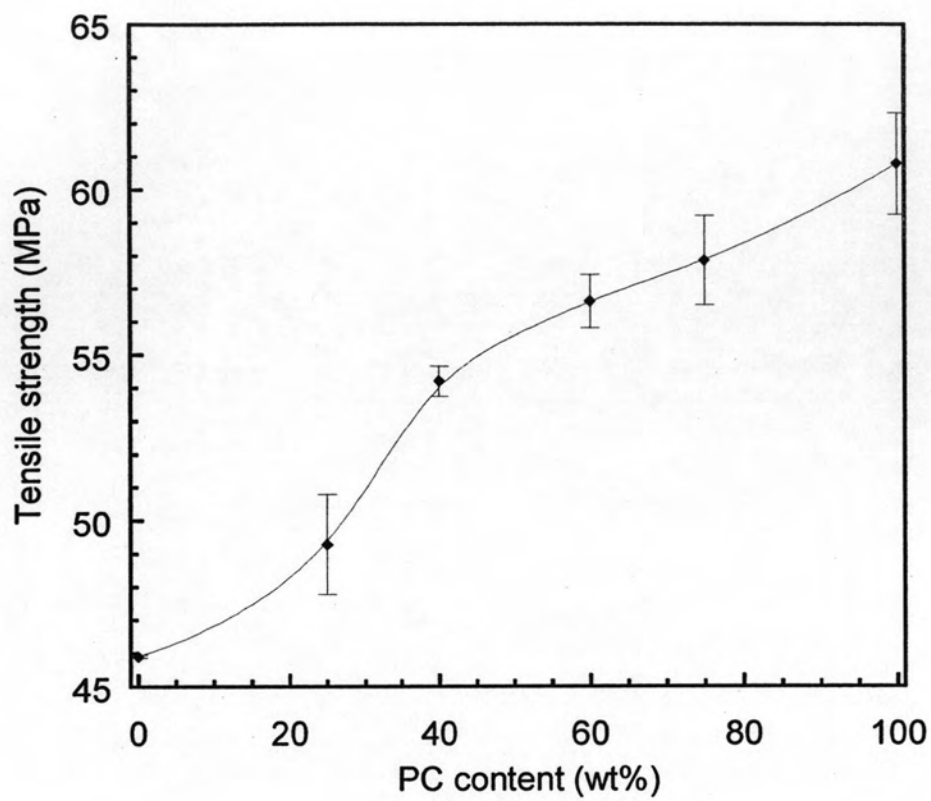
Figure 5.5: Tensile strength of PC/ABS blends as a function of PC content
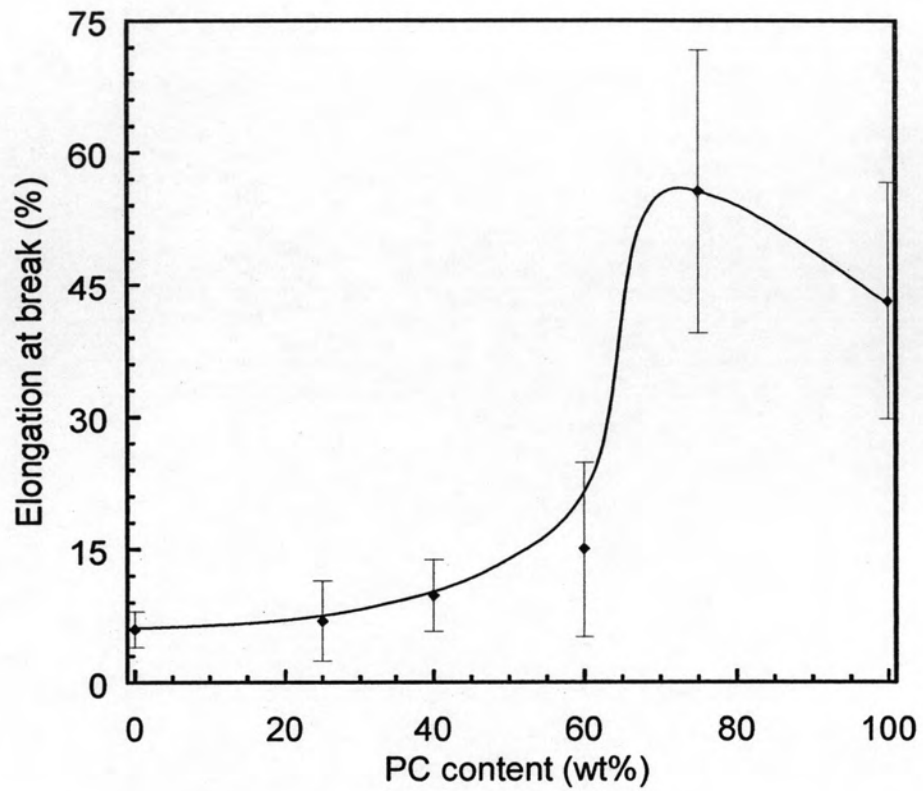
Figure 5.6: Elongation at break of PC/ABS blends as a function of PC content
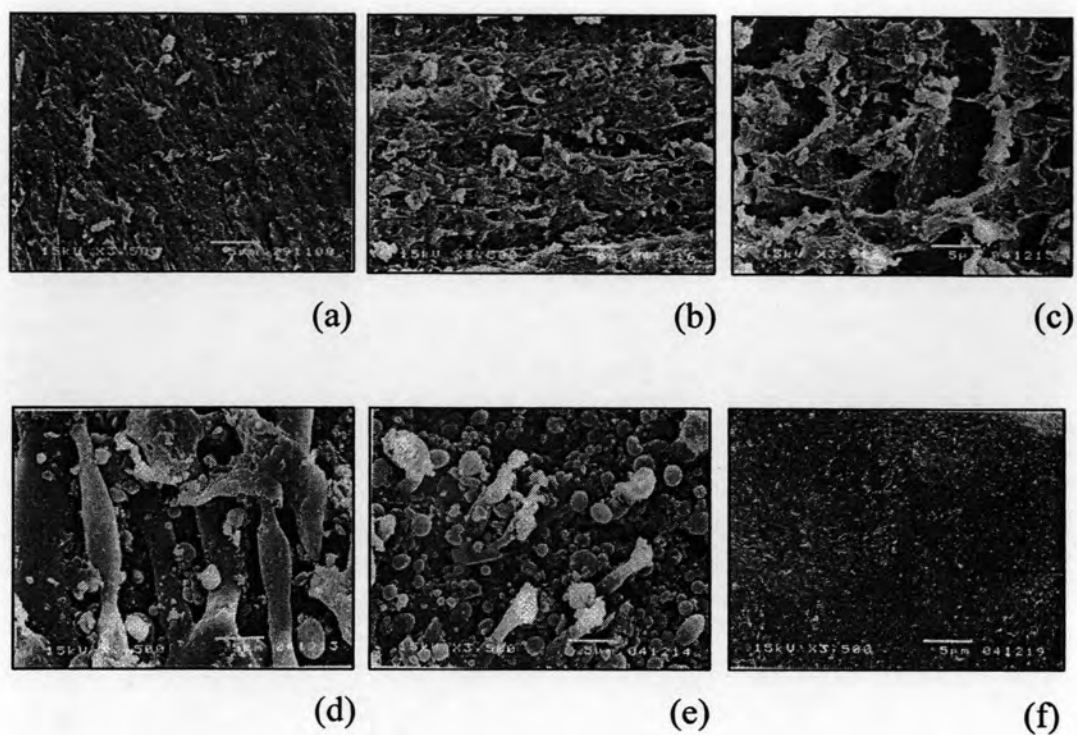
Figure 5.7: SEM micrographs of PC/ABS blends etched with a NaOH aqueous solution at various compositions : (a) pure ABS, (b) 25/75 PC/ABS, (c) 40/60 PC/ABS, (d) 60/40 PC/ABS, (e) 75/25 PC/ABS, and (f) pure PC
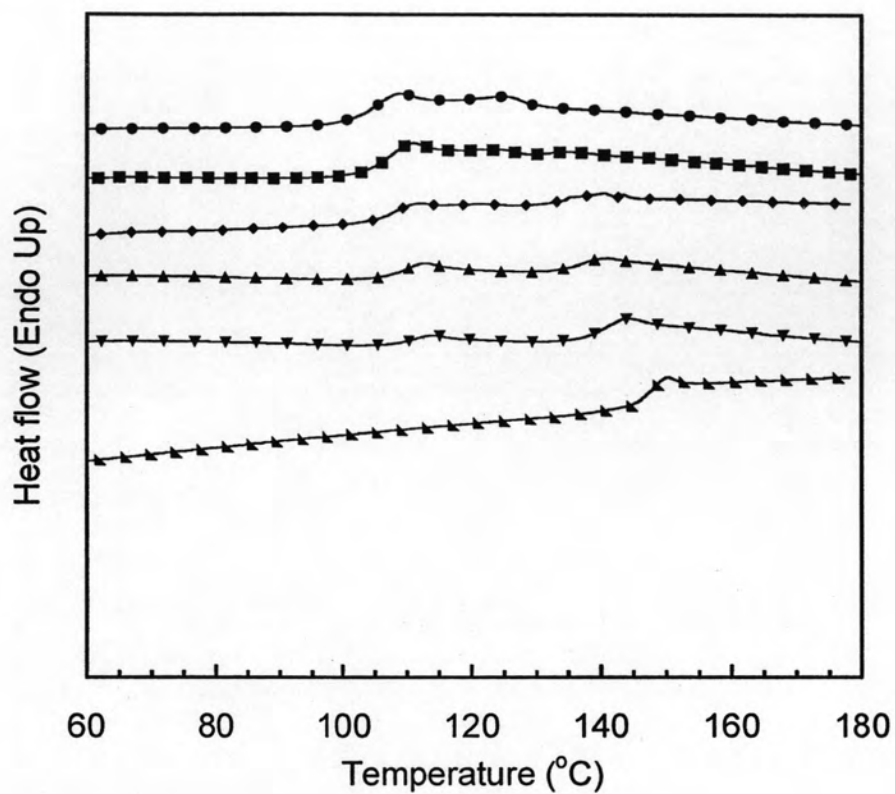
Figure 5.8: DSC thermograms of PC/ABS blends at various compositions: (●)ABS, (■)25/75, (♦)40/60, (▲)60/40, (▼)75/25, (◣)PC

**Table 5.2**: DSC thermograms of PC/ABS blends at various compositions

wt% PC	Tg of ABS rich phase (°C)	Tg of PC rich phase (°C)	PC fraction in ABS rich phase	ABS fraction in PC rich phase
0	104.47		0	
25	106.63	132.91	0.07	0.26
40	107.59	134.85	0.01	0.23
60	109.6	136.85	0.17	0.19
75	110.47	140.25	0.19	0.12
100		147.44		0
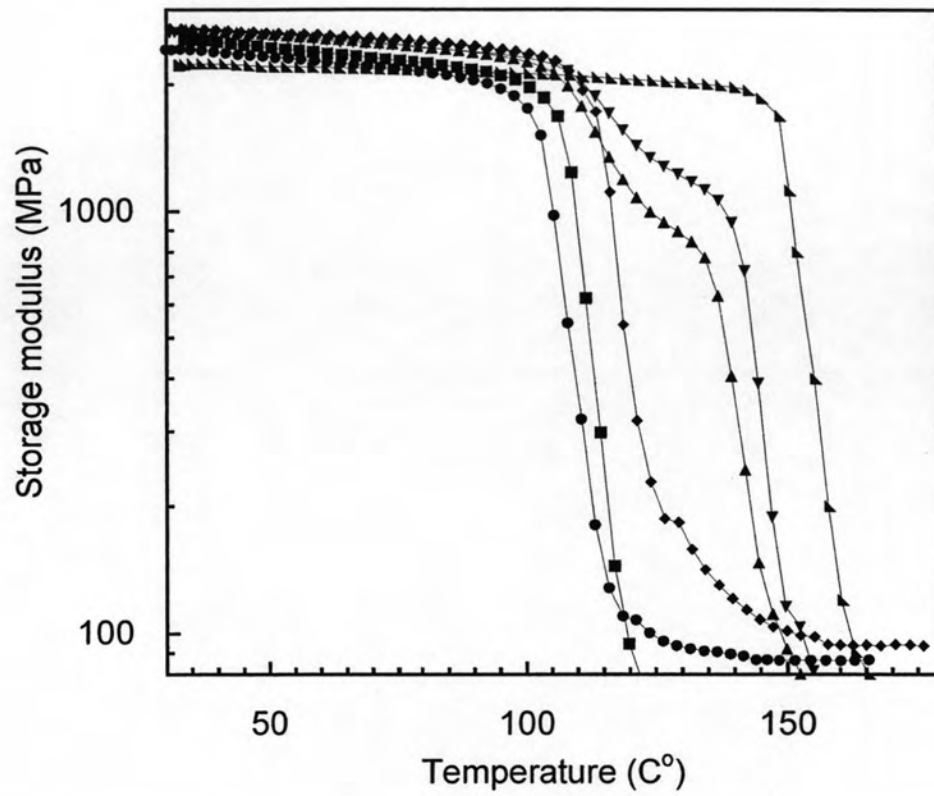
Figure 5.9: Storage modulus of PC/ABS blends at various compositions
: (●)ABS, (■)25/75, (◆)40/60, (▲)60/40, (▼)75/25, (◤)PC
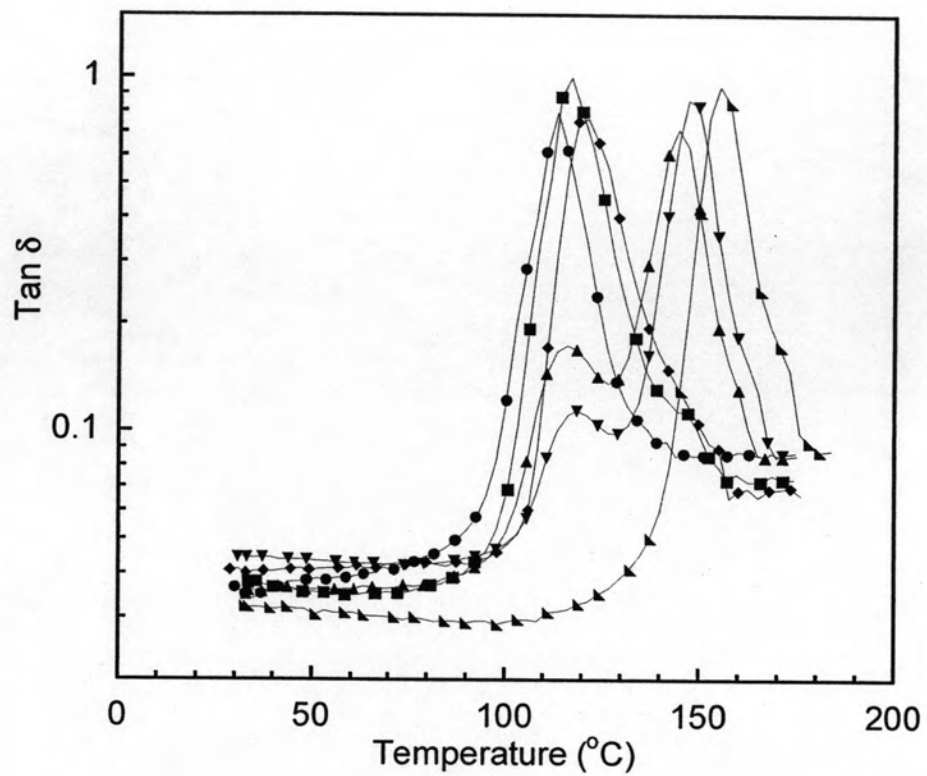
Figure 5.10: Tan δ of PC/ABS blends at various compositions: (●)ABS, (■)25/75, (◆)40/60, (▲)60/40, (▼)75/25, (◤)PC
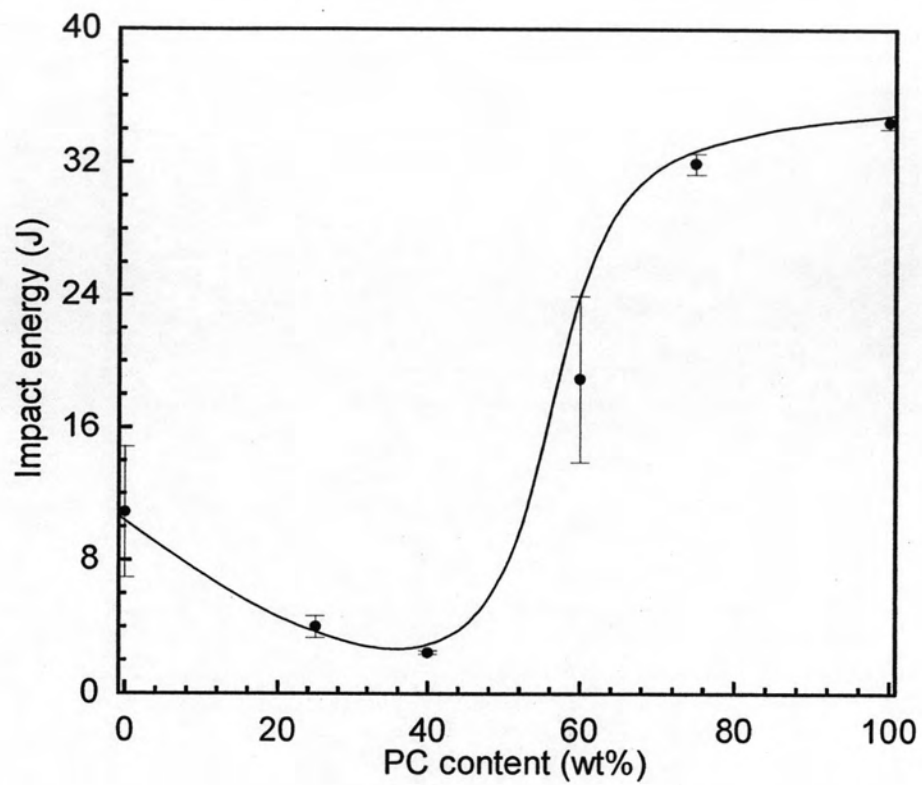
Figure 5.11: Relationship between the impact energy and PC content in PC/ABS blend
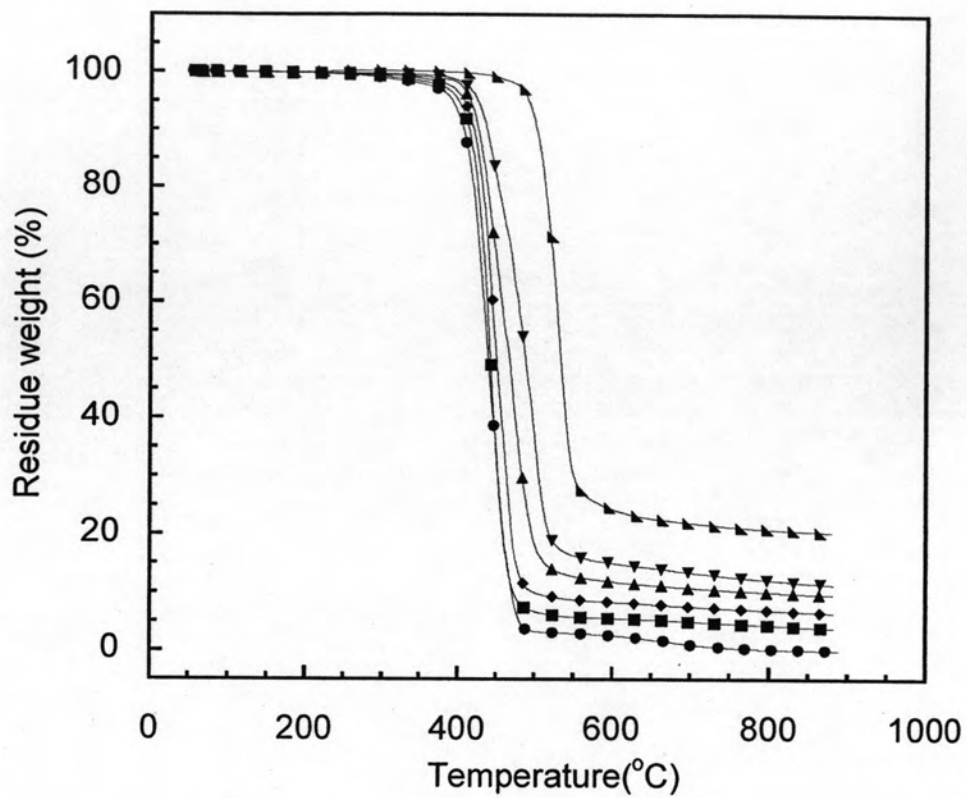
Figure 5.12: TGA thermograms of PC/ABS blends at various

Compositions: (●)ABS, (■)25/75, (◆)40/60, (▲)60/40,

(▼)75/25, (◣)PC
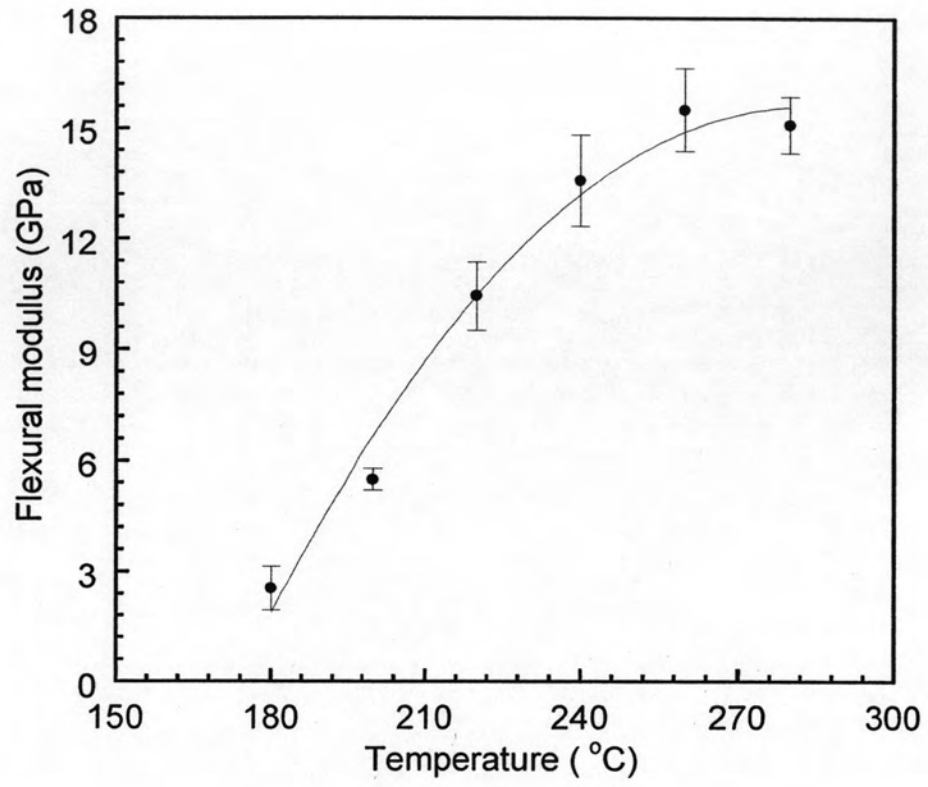
Figure 5.13: Flexural modulus of the composites at various hot pressing temperatures under a constant pressing pressure and time
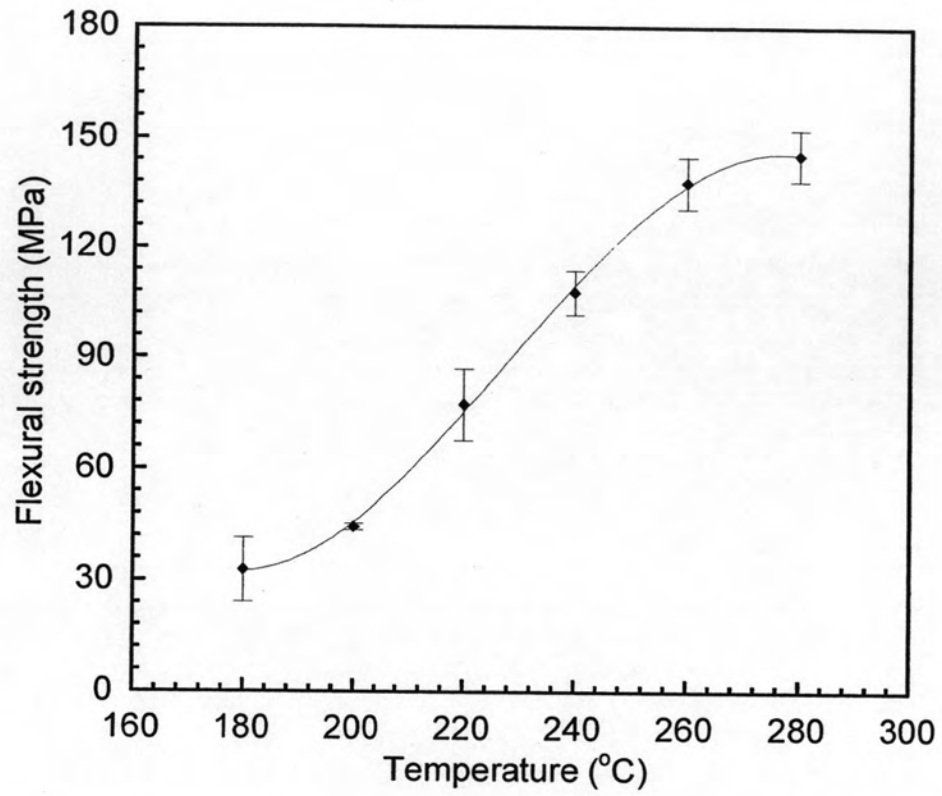
Figure 5.14: Flexural strength of the composites at various hot pressing
temperatures under a constant pressing pressure and time
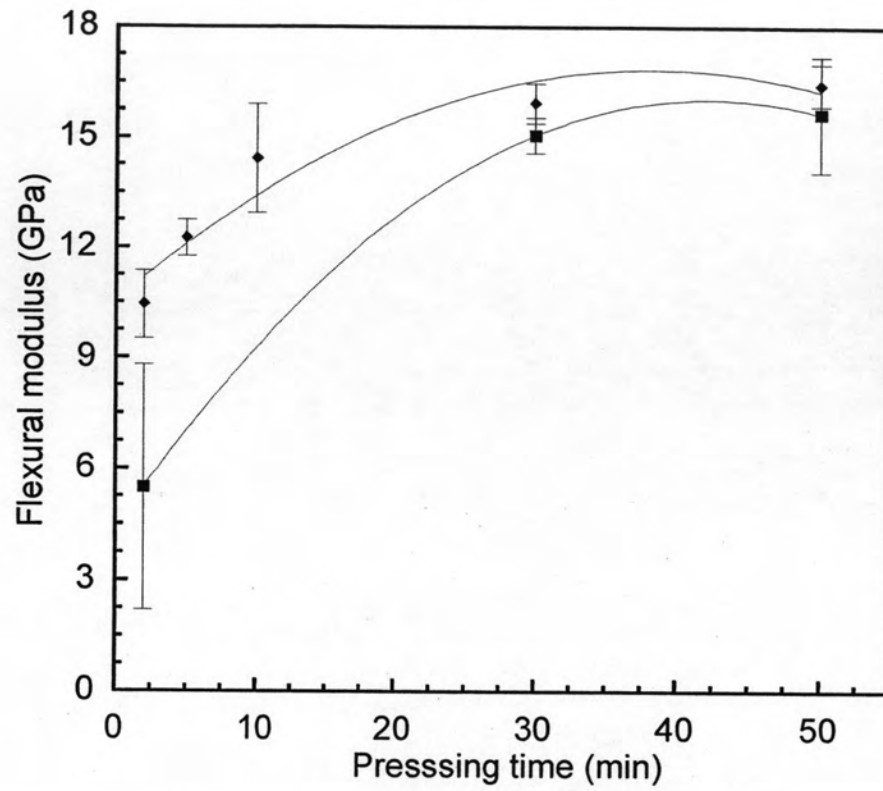
Figure 5.15: Flexural modulus of the composites processed at the
temperature of 200 and 220 °C at various times under
a constant pressure: (◆)220°C, (■)200°C
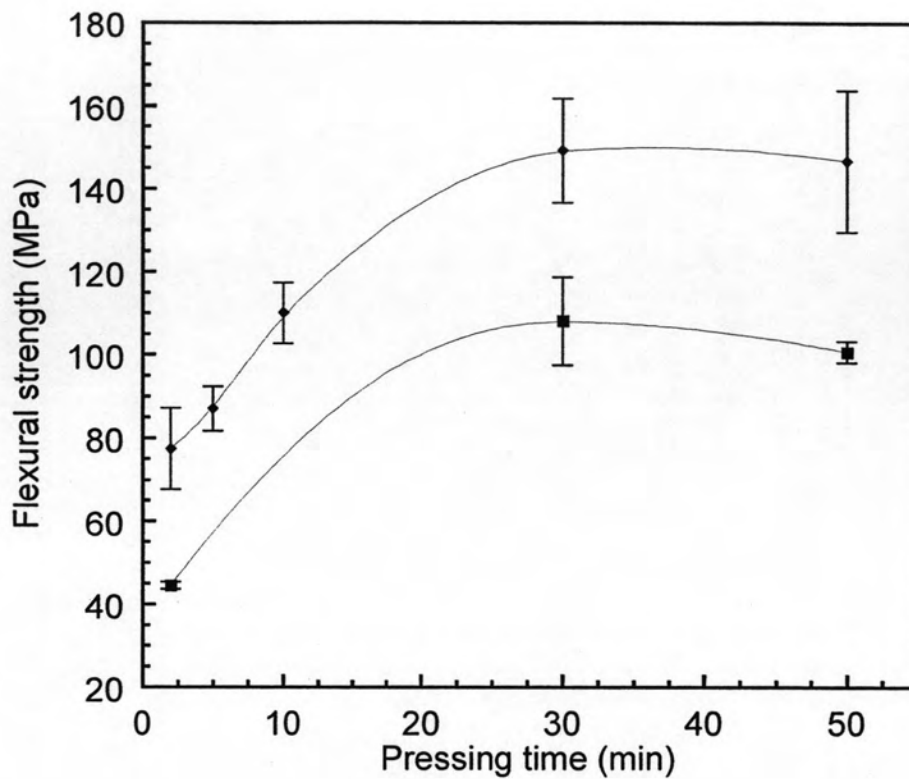
Figure 5.16: Flexural strength of the composites processed at the
temperature of 200 and 220 °C at various times under
a constant pressure: (◆)220°C, (■)200°C
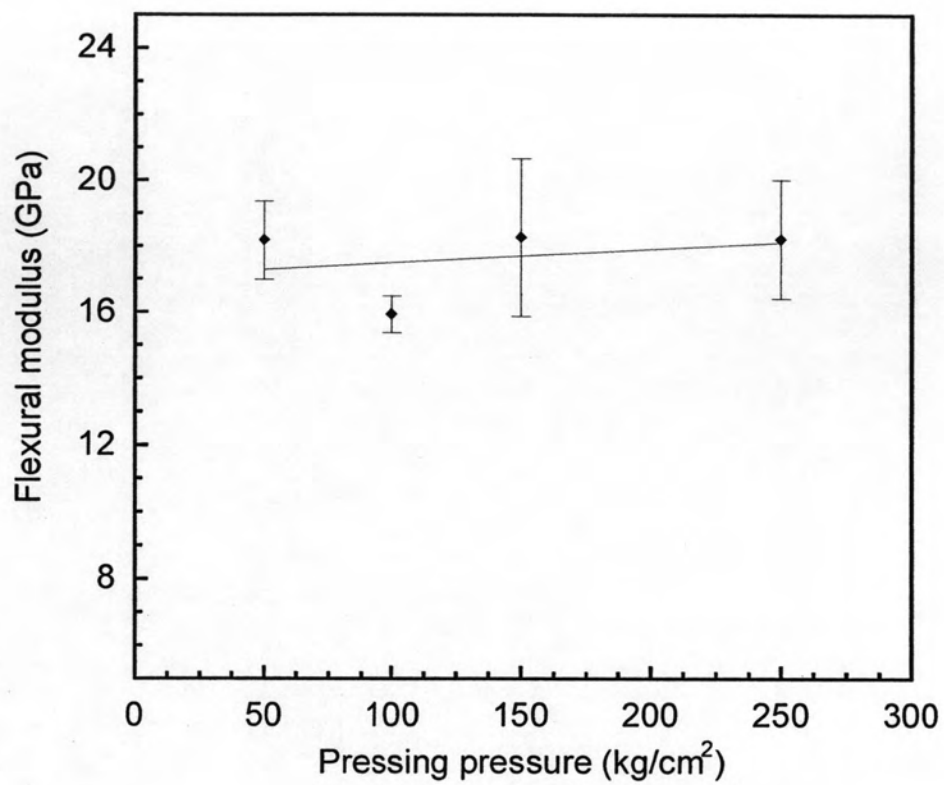
Figure 5.17: Flexural modulus of the composite processed at 220°C for 30 minutes using various pressing pressures
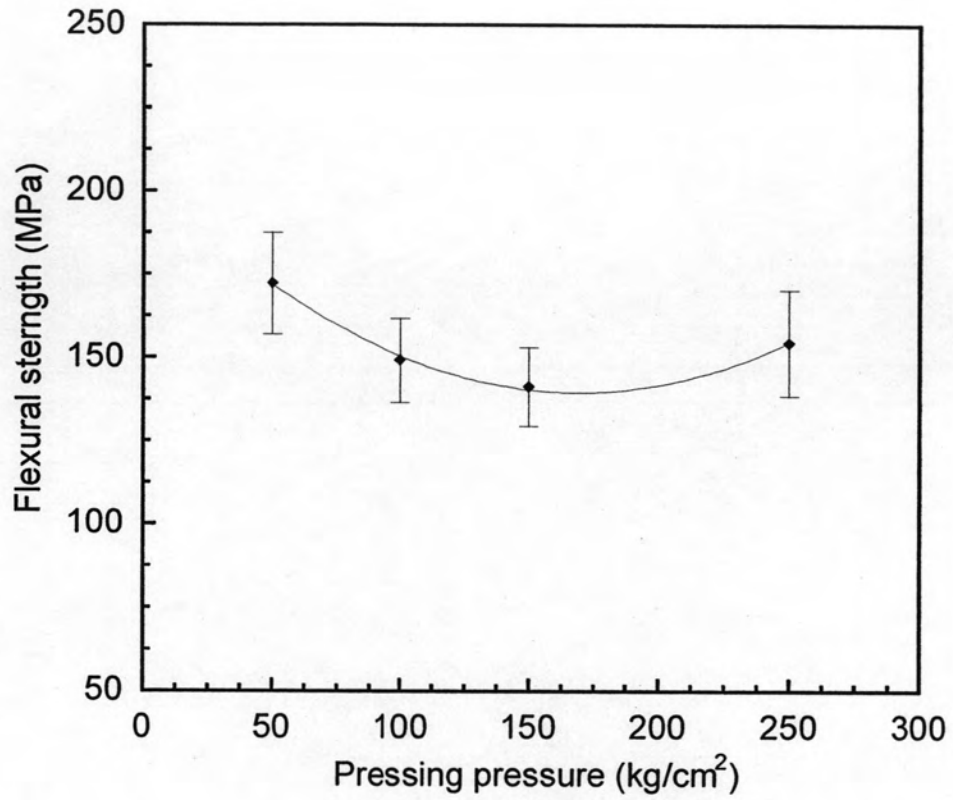
Figure 5.18: Flexural strength of the composite processed at 220°C for 30 minutes using various pressing pressures
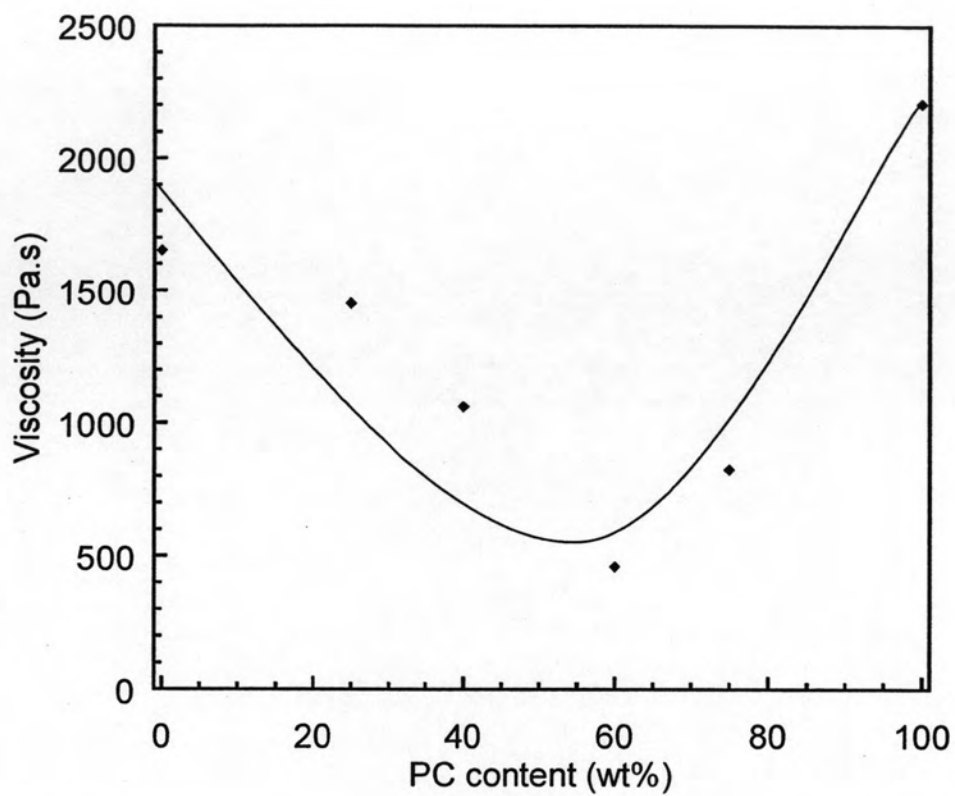
Figure 5.19: Melt viscosity at 260°C and constant shear rate (1 sec^{-1}) of PC/ABS blend as a function of PC content
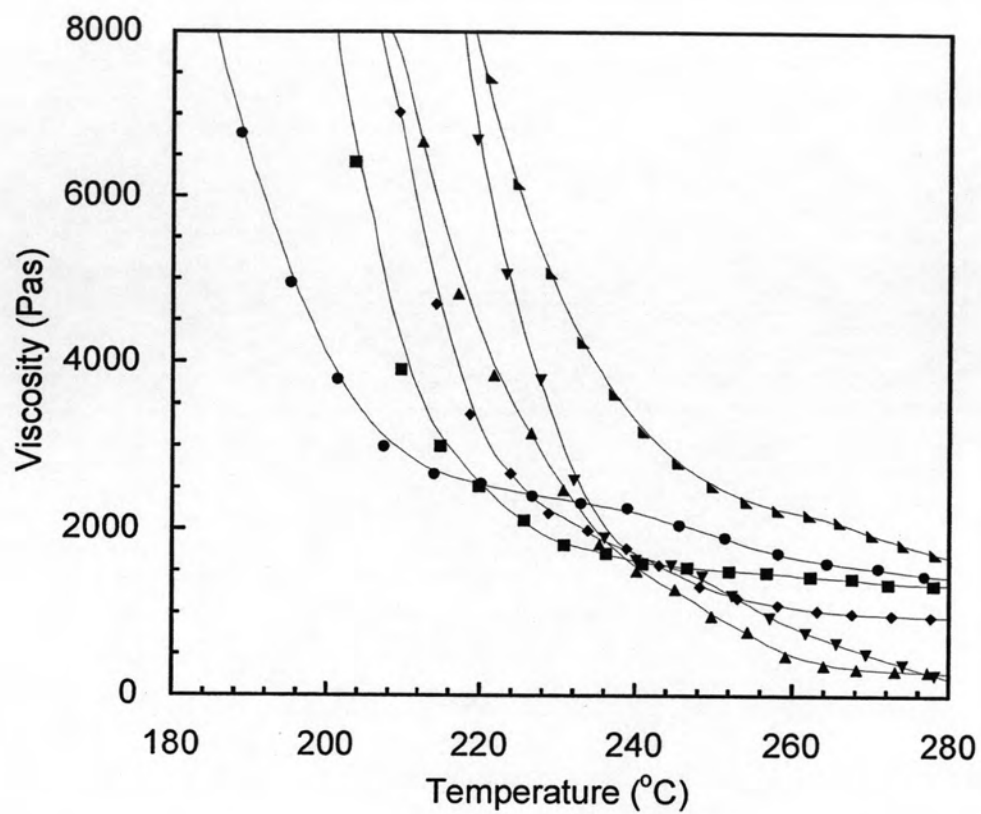
Figure 5.20: Variation in viscosity of PC/ABS blends measured over the temperature range of 160 to 280°C and constant shear rate at 1 sec⁻¹: (●)ABS, (■)25/75, (♦)40/60, (▲)60/40, (▼)75/25, (◤)PC

**Table 5.3**: Processing conditions of the composites at various matrix compositions

Composite	Temperature (°C)	Pressure (kPa)
ABS	200	250
25/75	208	250
40/60	216	250
60/40	220	250
75/25	225	250
PC2800	233	250

**Table 5.4**: Measured density and theoretical density of the composites with various matrix contents

| Film's Thickness (mm)	Matrix Content (wt%)	Fiber Content (wt%)	Theoretical Density (g/cm3)	Actual Density (g/cm3)
30	16.70	83.30	1.37	1.1090
40	19.25	80.75	1.36	1.1548
50	26.95	73.05	1.33	1.1925
100	33.47	66.53	1.31	1.1831
150	46.91	53.09	1.27	1.1535
200	52.19	47.81	1.26	1.1520
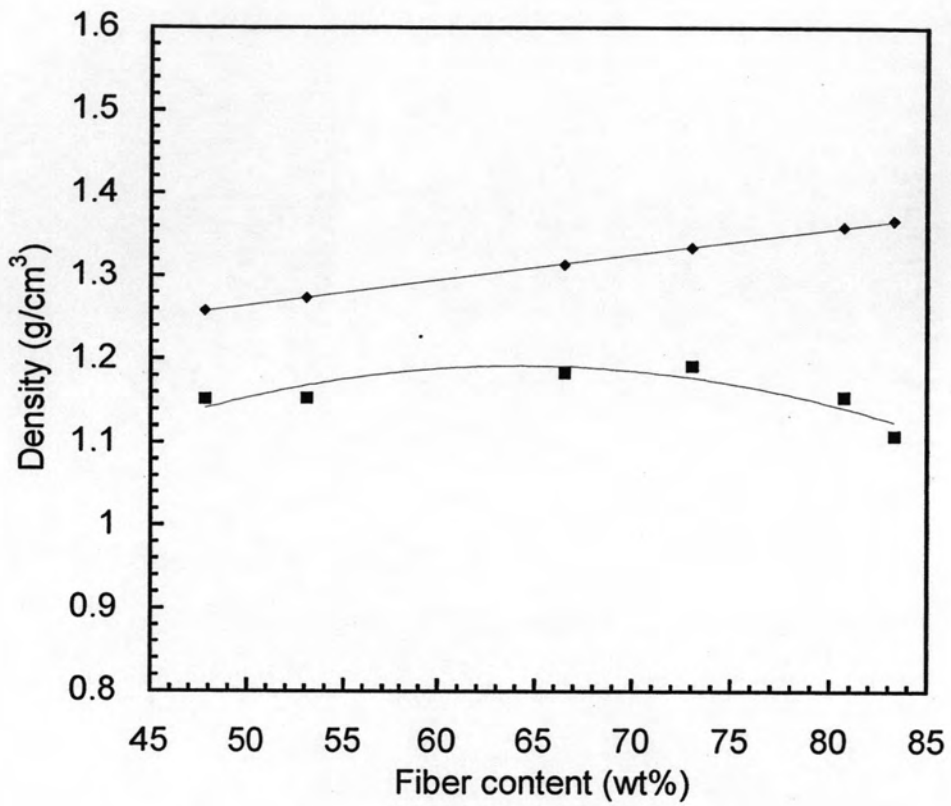
Figure 5.21: Comparison between the measured density and theoretical

density of the composite at various fiber contents
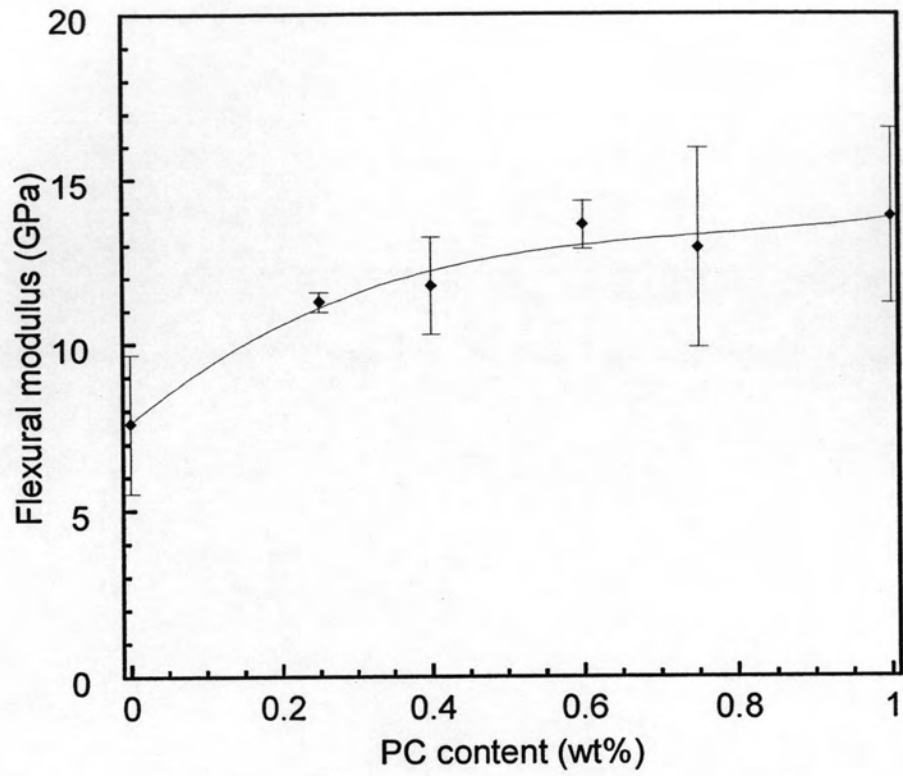
: (♦)Theoretical density, (■)Actual density
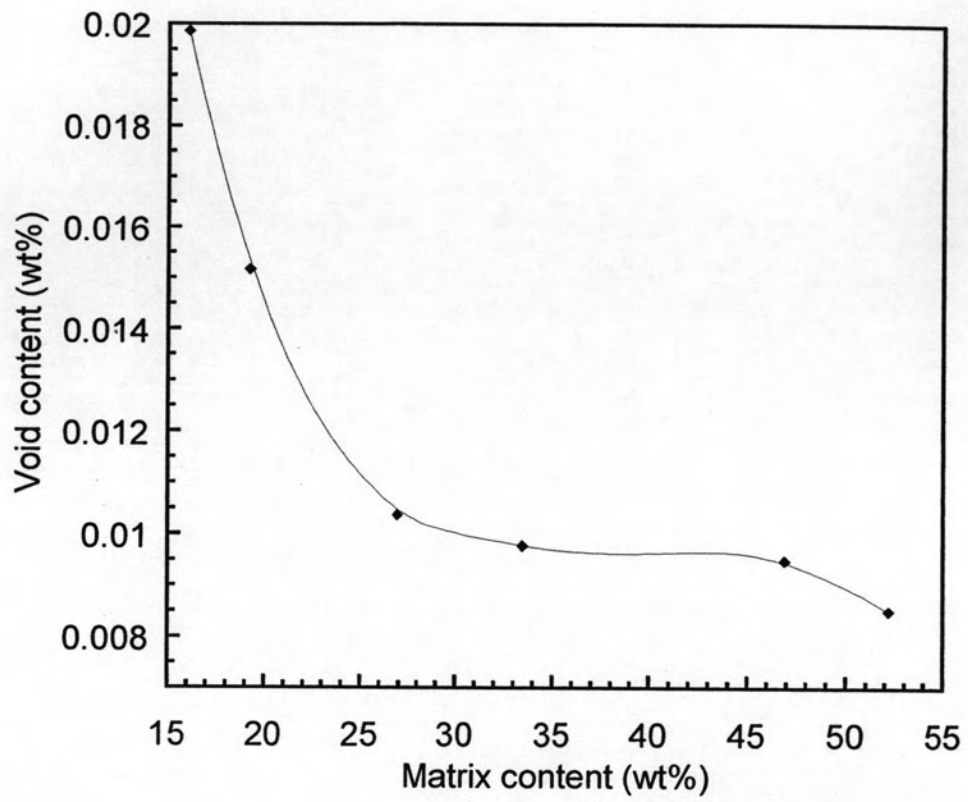
Figure 5.22: Calculated void content of the composite at various matrix
contents
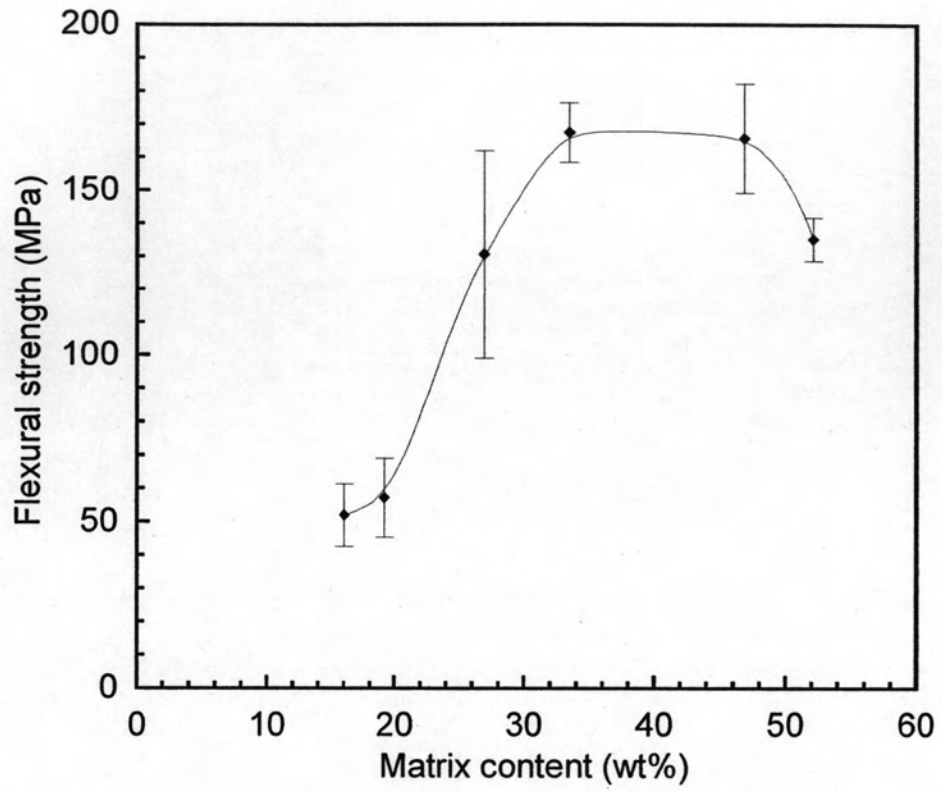
Figure 5.23: Flexural strength of Kevlar/PC/ABS composite as a
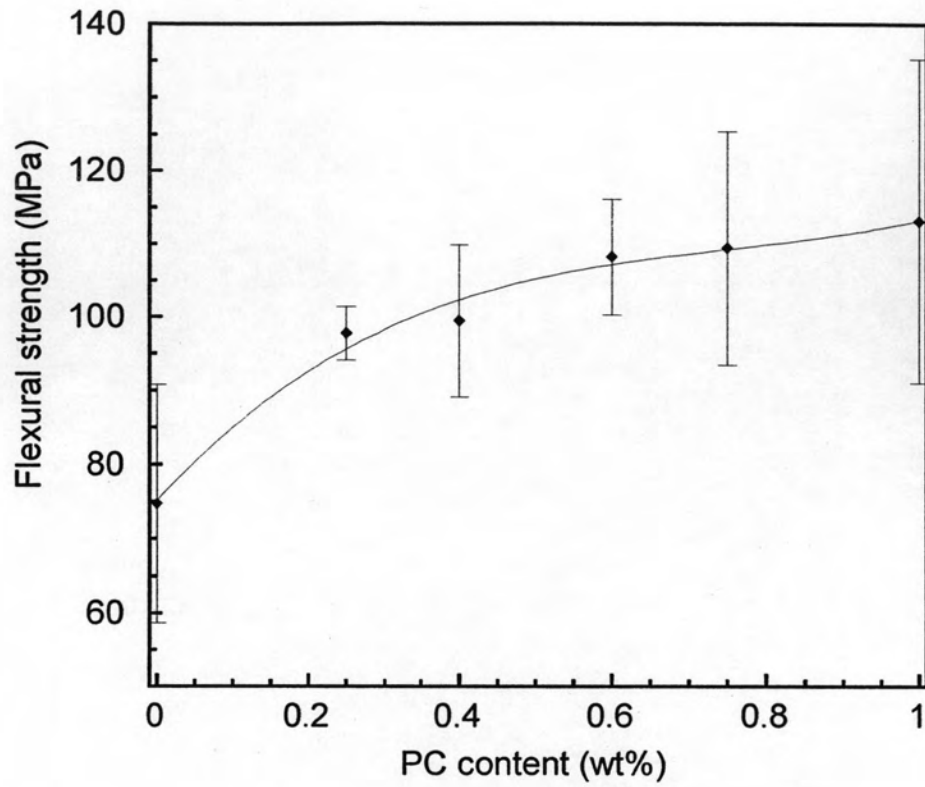
function of matrix content
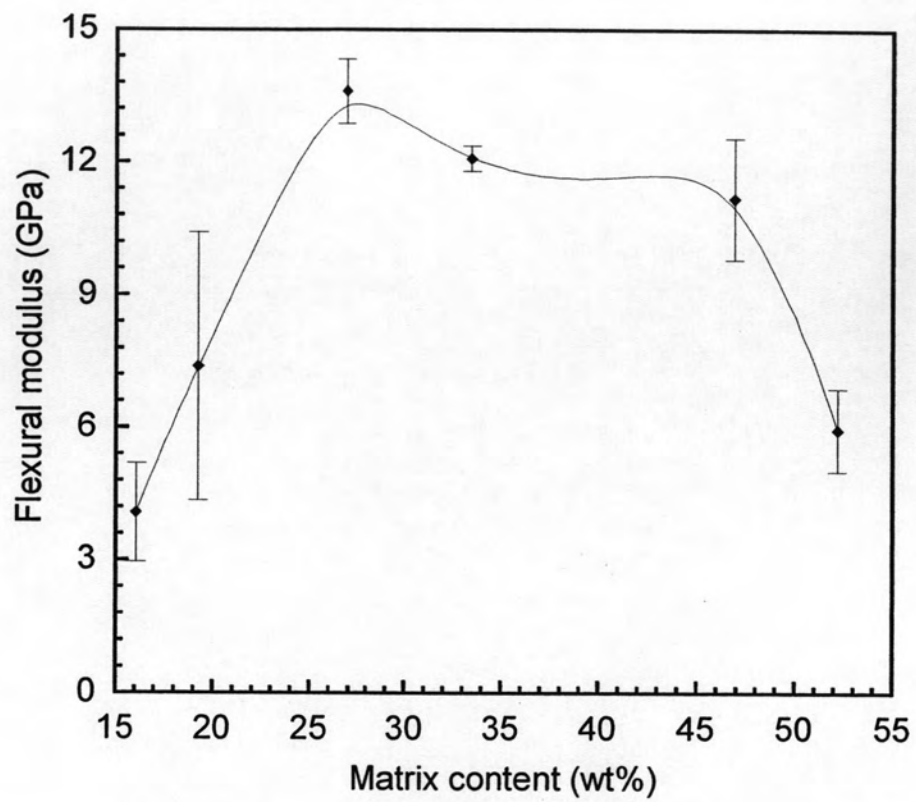
Figure 5.24: Flexural modulus of Kevlar/PC/ABS composite as a
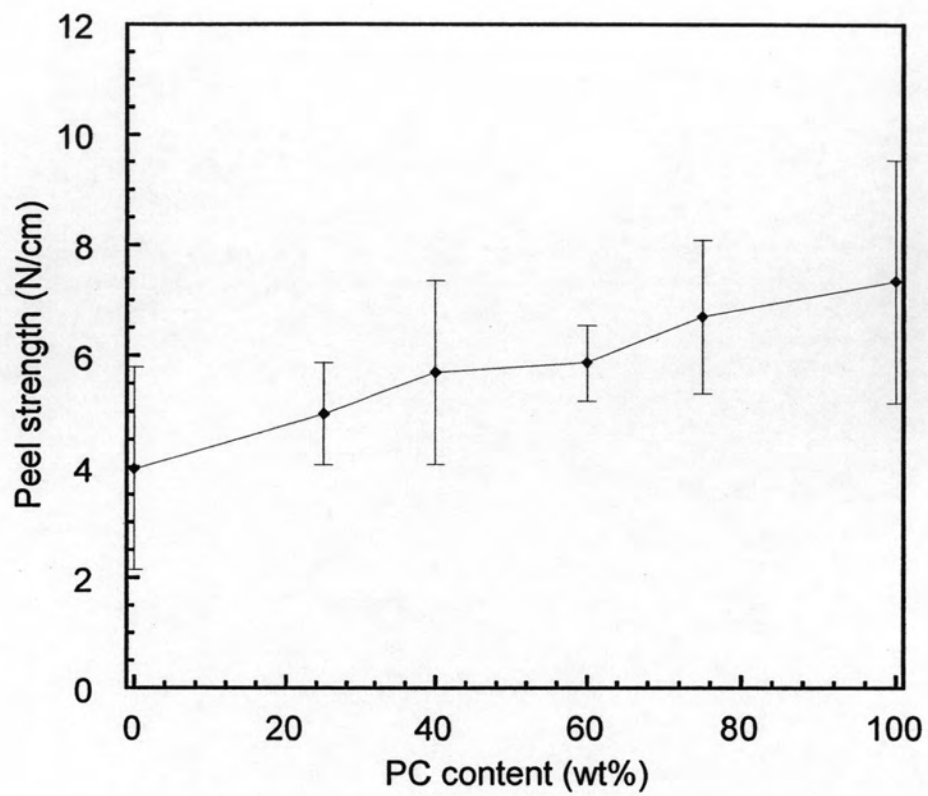function of matrix content

Figure 5.25: Flexural modulus of Kevlar-reinforced PC/ABS composites as a function of PC content in the matrix
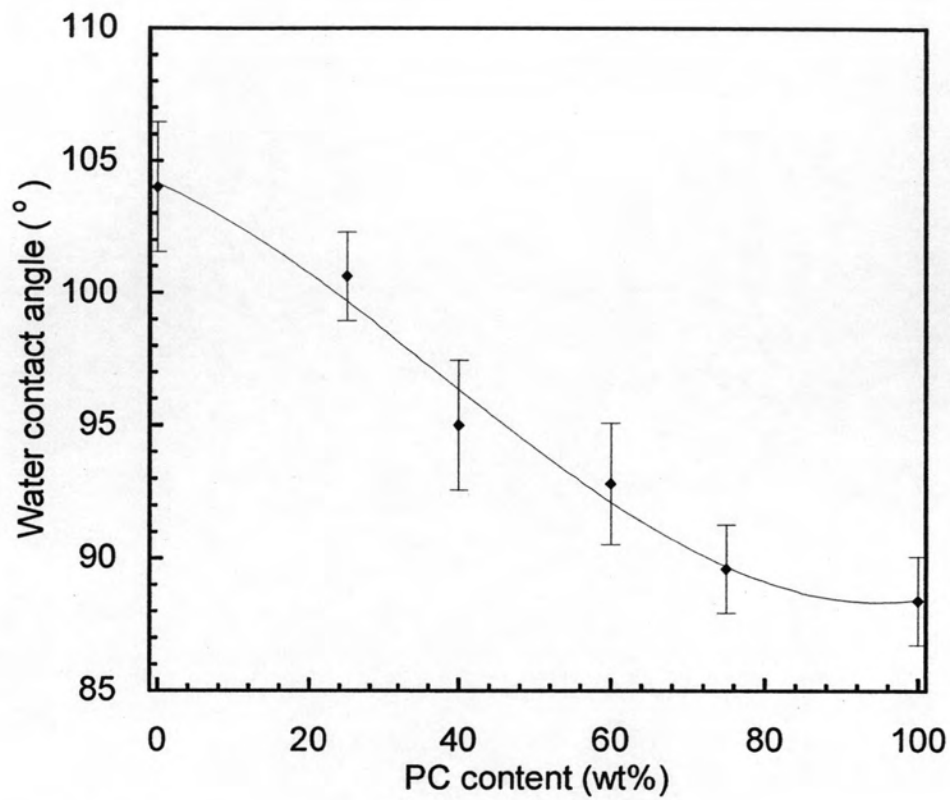
Figure 5.26: Flexural strength of Kevlar-reinforced PC/ABS composites as a function of PC content in the matrix

Figure 5.27: Peel strength of the composites as a function of PC content in the matrix

Figure 5.28: Variation in water contact angles of PC/ABS matrices at various compositions
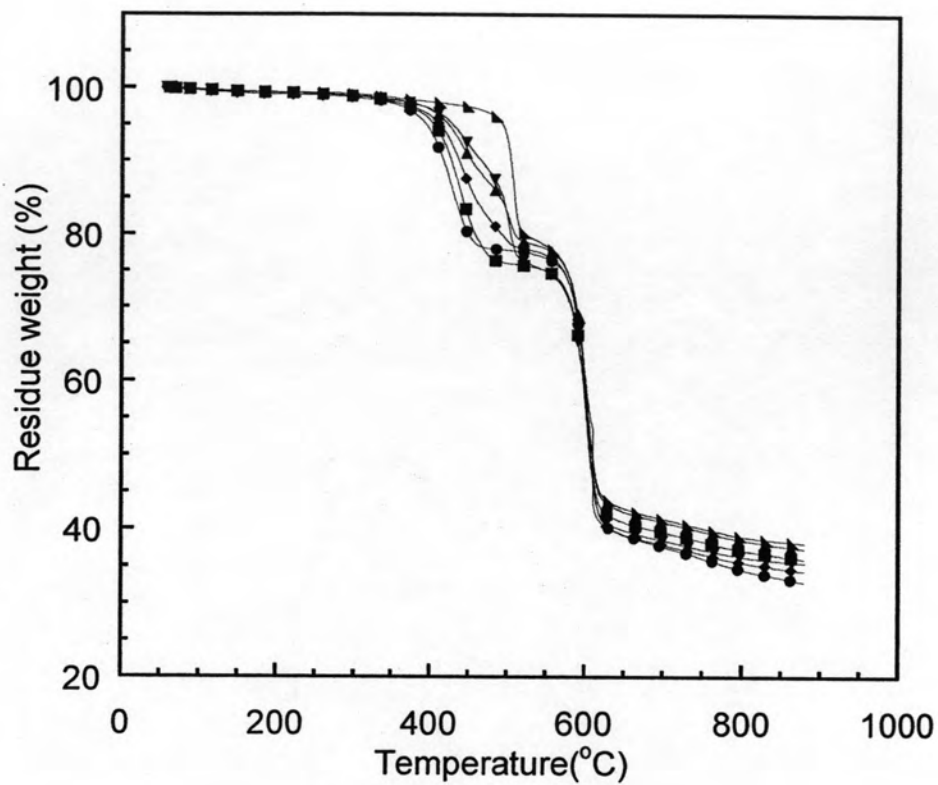
Figure 5.29: TGA thermograms of Kevlar-reinforced PC/ABS composites at various matrix compositions: (●)ABS, (■)25/75, (◆)40/60, (▲)60/40, (▼)75/25, (◤)PC

Table 5.5a: Low level ballistic impact test results of the composites at various matrix compositions

Number	Type of Matrix	Number of Plies Plate1+ Plate2	Resistance to Penetration	
			Front Plate	Rear Plate
1	ABS	10+10	Yes	Yes
2	ABS	10+10	Yes	Yes
1	25/75 PC/ABS	10+10	No	Yes
2	25/75 PC/ABS	10+10	No	Yes
1	40/60 PC/ABS	10+10	Yes	Yes
2	40/60 PC/ABS	10+10	Yes	Yes
1	60/40 PC/ABS	10+10	Yes	Yes
2	60/40 PC/ABS	10+10	Yes	Yes
1	75/25 PC/ABS	10+10	Yes	Yes
2	75/25 PC/ABS	10+10	Yes	Yes
1	PC	10+10	No	Yes
2	PC	10+10	No	Yes

Table 5.5b: Damage dimension of rear Plate of the composites with Low
level ballistic impact test

Type of Matrix	Number of Plies Plate1+ Plate2	Damage Dimension of Rear Plate of the Composite	
		Diameter (mm)	Depth (mm)
ABS	10+10	55.4	16.2
25/75 PC/ABS	10+10	63.3	23.0
40/60 PC/ABS	10+10	61.2	18.2
60/40 PC/ABS	10+10	59.0	19.3
75/25 PC/ABS	10+10	51.5	12.9
PC	10+10	48.8	18.3
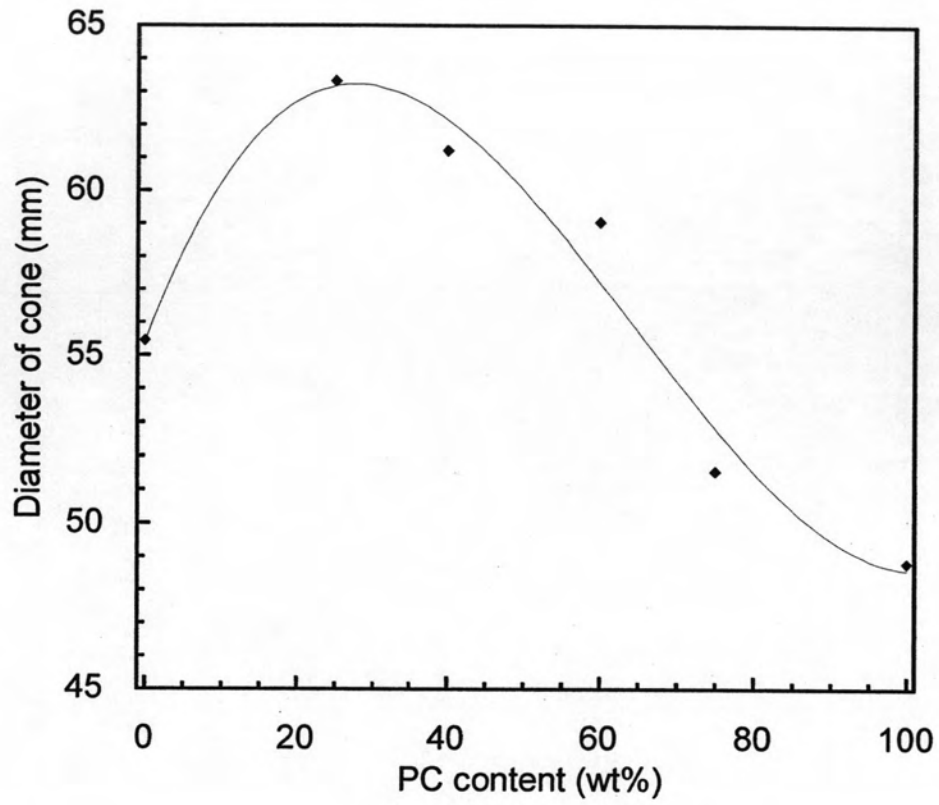
Figure 5.30: Diameter of after fired delamination area of the composites at various matrix compositions

**Table 5.6**: Wave velocities of the composite at various matrix compositions

Type of Matrix	Composite Modulus (GPa)	Composite Density (g/cm^3)	Wave Velocity (Km/s)
ABS	7.6	1.13	2.59
25/75 PC/ABS	11.2	1.19	3.07
40/60 PC/ABS	11.7	1.19	3.14
60/40 PC/ABS	13.5	1.21	3.35
75/25 PC/ABS	12.9	1.22	3.25
PC	13.8	1.25	3.33

Table 5.7: Damage volume of the clay witness with Low level ballistic impact test

Type of Matrix	Number of plies Plate1+ Plate2	Damage Dimension of the Clay Witness		
		Diameter (mm)	Depth (mm)	Volume (ml)
ABS	10+10	61.5	24.0	42.5
25/75 PC/ABS	10+10	64.4	30.7	61.0
40/60 PC/ABS	10+10	61.5	22.6	31.5
60/40 PC/ABS	10+10	61.7	31.2	58.0
75/25 PC/ABS	10+10	71.3	27.3	51.0
PC	10+10	66.6	27.8	41.0

a) (X900)   c) (X900)   e) (X900)

b) (X250)   d) (X250)   f) (X250)
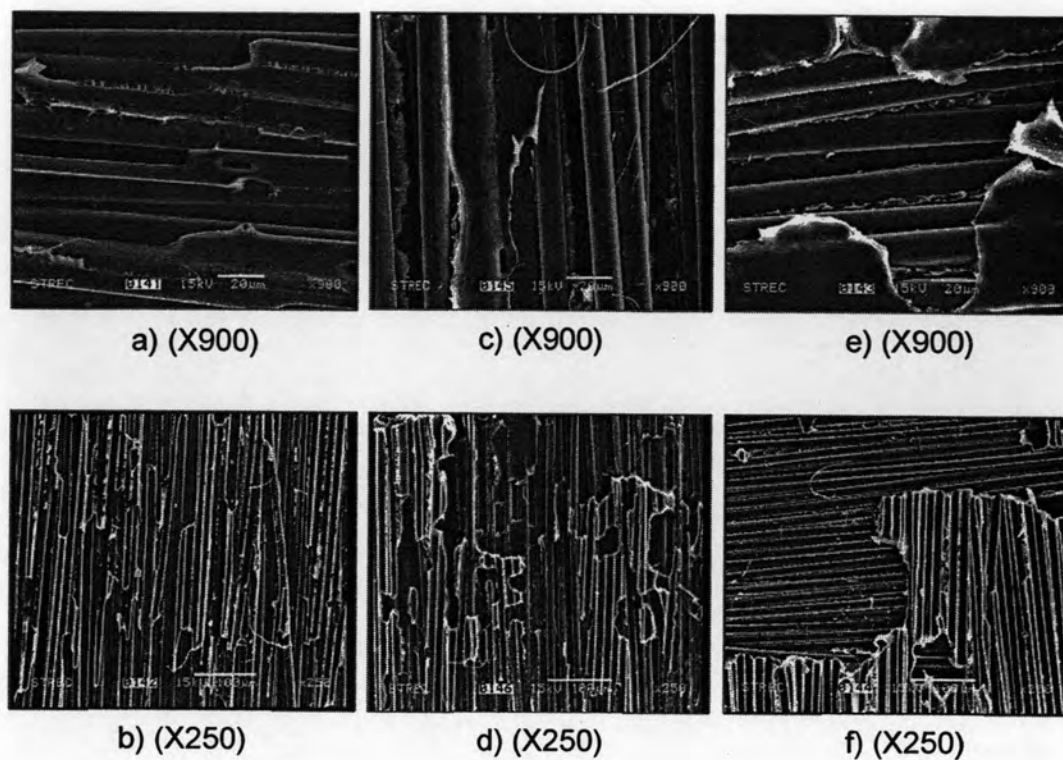
Figure 5.31: SEM micrographs of Kevlar/PC/ABS composites at various matrix compositions: (a,b) pure ABS, (c,d) 40/60 PC/ABS and (e,f) pure PC

Table 5.8: Effect of number of piles of Kevlar-reinforced 40/60 PC/ABS composite after ballistic impact with NIJ standard level IIIA

Number of Layers of Composite	Impact Velocity (m/s)	Resistance to Penetration		Damage Dimension of the Clay Witness	
		1st	2nd	Diameter (mm)	Depth (mm)
30+10 +10+10	427.8	Yes	Yes	84.6	31.9
30+10 +10	427.7	Yes	Yes	95.4	34.9
30+10	437.9	No	-	-	-
40	418.1	No	-	-	-

Table 5.9: Effect of panel arrangement of Kevlar-reinforced 40/60
PC/ABS composite after ballistic impact with NIJ standard
level IIIA

Number of Layers of Composite	Impact Velocity (m/s)	Resistance to Penetration	Damage Dimension of the Clay Witness	
			Diameter (mm)	Depth (mm)
20+10+10+10	416.9	Yes	95.3	38.5
30+10+10	427.7	Yes	95.4	33.9
40+10	412.9	Yes	94.5	34.5
50	425.1	Yes	95.6	35.5